5-1-2013

Design and Testing of Novel Mouthguard with Intermediate Nitinol and Foam Layers

Adam Kessler
University of Nevada, Las Vegas, kesslera@unlv.nevada.edu

DESIGN AND TESTING OF NOVEL MOUTHGUARD WITH INTERMEDIATE NITINOL AND FOAM LAYER

By

Adam Samuel Kessler

Bachelor of Science in Mechanical Engineering
University of California, Berkeley
2000

A thesis submitted in partial fulfillment
of the requirements for the

Master of Science in Mechanical Engineering

Department of Mechanical Engineering
College of Engineering
The Graduate College

University of Nevada, Las Vegas

May 2013

THE GRADUATE COLLEGE

We recommend the thesis prepared under our supervision by

Adam Samuel Kessler

entitled

Design and Testing of Novel Mouthguard with Intermediate Nitinol and Foam Layers

be accepted in partial fulfillment of the requirements for the degree of

Master of Science in Mechanical Engineering
Department of Mechanical Engineering

Brendan O'Toole, Ph.D., Committee Chair

Mohamed Trabia, Ph.D., Committee Member

Hui Zhao, Ph.D., Committee Member

James Mah, D.D.S, Graduate College Representative

Thomas Piechota, Ph.D., Interim Vice President for Research &
Dean of the Graduate College

May 2013

ABSTRACT

It is the aim of this study to investigate a novel mouthguard design that incorporates the use of a nickel-titanium (Nitinol) layer and thin foam layer in addition to EVA layers. It is thought that the Nitinol layer can distribute the force of an impact and that the thin foam layer may absorb this distributed force better than a solid EVA mouthguard of the same thickness. Rectangular, flat coupons representative of several mouthguard configurations were constructed for testing using an instrumented drop-weight impact tower. The coupon configurations include a control made of laminated EVA, a group of laminated EVA and Nitinol, laminated EVA and foam, and a group of laminated EVA with foam and Nitinol. Several thicknesses of EVA were used in each configuration as well as three different Nitinol insert designs. The construction and subsequent testing of the coupons was performed in conjunction with the UNLV School of Dental Medicine.

Two test methods were used to evaluate the coupons using the drop tower machine. The first test involved dropping a mass onto the coupon supported by a flat plate attached to a load cell. The second test involved dropping the mass onto the coupon resting on a simply supported beam attached to a load cell. The metric by which the coupons are evaluated are peak forces transmitted to the load cell, and strain (or deflection) experienced by the simply supported beam in the case of the second test. The energy absorbed by the coupon was calculated using the strain energy in the beam at the

moment of peak force and deflection and performing an energy balance on the system. Measurements were normalized by thickness and compared to the control group.

While there were some improvements in performance with the novel design, these were only modest, and the group of designs using only Nitinol (no foam) actually performed worse than the control.

ACKNOWLEGMENTS

Special thanks to Freddie Martinez, D.D.S and David Jolly, D.D.S. for all their hard work creating and testing the hundreds of samples for this research. Thanks to Jagadeep Thota, Ph.D. for his help with the equipment used. Thanks also to Joan Conway for all of her help over the last three years in navigating the university. And thanks to professors Dr. James Mah and Dr. Brendan O'Toole for their guidance. Finally, thanks to my parents for their patience, flexibility and support.

TABLE OF CONTENTS

LIST OF FIGURES

CHAPTER 1

INTRODUCTION

Background

Mouthguards are a common fixture in the realm of modern athletics, and are employed in a variety sports including boxing, American football, basketball, hockey and MMA. The device is intended to reduce the likelihood and severity of several orofacial injuries during an impact event. The opportunities for orofacial injury during sport are numerous, and lead, not only, to pain experienced by the athlete, but cost incurred by the athlete due to dental work required to repair the damage caused by an impact. Another concern is brain concussion resulting from impact forces via the jaws to the brain. To illustrate the prevalence of orofacial injury during sporting events, a study was conducted in 2007 at the Pan American Games, in which 49.6% of a sample group of 409 athletes suffered some kind of dental trauma (Andrade, et al., 2010). Also detailed in this study is that over two-thirds of the participants who incurred traumatic lesions were not wearing mouthguards. For reasons like this, mouthguards are now required equipment in several amateur and professional sports (Knapik, et al., 2007)

Since its introduction in the 1920's, the mouthguard has taken on a variety of forms, but the most common mouthguards take on one of three forms; stock, boil-and-bite and custom (Patrick, van Noort, & Found, 2005). The American Society of Materials Testing (ASTM) recognizes this and actually classifies the three types of mouthguards as: type I, stock; type II, mouth-formed, and type III, custom fabricated

over a model (ASTM F697-80). Stock mouthguards come in different sizes and are ready to use, made of polyurethane, or a co-polymer of vinyl acetate or ethylene. Mouth formed, or boil-and-bite mouthguards are formed to the user by first heating the guard (in boiling water) and biting and sucking the guard until it cools and conforms to the user. Custom made mouthguards are made in a dental laboratory on a cast of the user's maxillary. The mouthguard material is heated and formed to the cast using specialized equipment.

The degrees to which each type of mouthguard protects the user depend on how well the guard fits, and the material it is made of. The degree of protection is generally correlated to the cost of the mouthguard. The cheapest, stock mouthguards, give poor retention, and are held in place by holding the teeth closed, and the best retention is afforded by the custom guards, which are relatively expensive (Oikarinen, Salonen, & Korhonen, 1993). The custom fit guards attract attention in a lot of the work done by researchers in this field due to the relatively high degree of protection they can provide, and the ability to improve a custom mouthguard with newer and better designs.

The shape, or fit to the user, is just one variable that affects the performance of a mouthguard. The material of which the mouthguard is made also affects the performance of the mouthguard. Several materials are commercially available for making custom mouthguards, such as Pro-form™, Poly-shock™ and Bioplast™. Studies have been performed to evaluate the shock absorbing potential of these different materials whether test samples of the materials are used or fully formed custom mouthguards are used. The results of these studies are fairly straight-forward, and provide the dental professional

with information to choose the material that he/she sees fit for the particular user for whom they are making a mouthguard. What may not be so straight-forward is testing of different mouthguard designs; that is, what type of construction may give the best protection to the user. At this point, the stock and boil-and-bite mouthguards may be left alone as their material and construction is controlled by the manufacturer, and leaves little control to the dental professional. But in the realm of custom mouthguards, the dental professional has much more room to design and customize a mouthguard tailored to each individual patient. It is here that variations to the construction and use of materials can have a great impact on performance and many studies explore optimizing mouthguards using the latitude afforded in custom guards. It is also here that the matter of testing these different designs presents a challenge.

Proposal

The aim of this study to investigate a novel mouthguard design that incorporates the use of a nickel-titanium (Nitinol) layer and thin foam layer in addition to ethylene vinyl acetate (EVA) layers. It is thought that the Nitinol layer can distribute the force of an impact and that the thin foam layer may absorb this distributed force better than a solid EVA mouthguard of the same thickness. The design of this novel mouthguard is explained more thoroughly in chapter two, but it basically involves using commercially available materials and laminating a metallic layer and a foam layer between them to better distribute and absorb the shock of an impact. This design would be constructed in a similar manner to a custom mouthguard by heating layers EVA, and laminating between these layers a Nitinol insert and a foam layer. The Nitinol insert and the foam would be designed to cover the central and lateral incisors of the maxillary (front teeth),

while the rest of the mouthguard would consist of EVA alone. In order to test the design, several rectangular coupons representative of the design will be tested along with coupons representing different components of the design (i.e. the foam or the Nitinol insert alone). But before this is presented, it is important to look at what has been done before, what ideas seem to work and how they are evaluated.

What follows in the following sections are several studies that present testing of materials used in mouthguards and several studies that explore different designs, all aimed at finding the best mouthguard. The test design and metric used to evaluate each different design or material is also noted and evaluated because it will relate to the research presented in later chapters.

Previous Studies

The fact that the design and construction of mouthguards is truly important has not been lost on the community of dental professionals and academics. The focus of these studies have different concentrations varying from identifying the optimal thickness of a mouthguard to the optimal material from which to make them, and even to the investigation of integrating different layers of materials into the mouthguard. Whatever the concentration of the study, the goal is to identify the best performing design and construction; however, the test design and metric by which the mouthguard is evaluated varies. The test methods used can usually be divided into two groups: those that employ the use of a pendulum impact object which strikes the mouthguard, and those that use some kind of a falling object that impacts the mouthguard. In the case of a pendulum impact object, either the pendulum head or the mouthguard is outfitted with a force

sensor in one way or another. In the case where a falling object is used to strike the mouthguard, the force sensor is typically located beneath the guard. Whatever test method is employed, some measurement, or metric, must be identified as a way to evaluate the performance of the mouthguard. In some tests, the peak force recorded by the force sensor is used as the metric, and this is typical for tests employing a pendulum impact object. In other tests energy absorption is used as the metric, and is typically measured by the difference between initial height and rebound height of the dropped mass. In some tests, the impulse force is used as a metric by integrating the data from the force sensor over the time of the impact. Several studies investigating the performance of mouthguards are summarized below. The summaries only cover the material as it relates to shock absorption ability of the mouthguards, as this will be the concentration of this thesis.

Park, 1994

Park performed a study to evaluate several aspects of a mouthguard performance including water absorption, density, tensile properties and energy absorption (Park, Shaull, Overton, & Donly, 1994). These tests were conducted due to the concern on the author's part that during processing of a boil-and-bite mouthguard, the material (namely, EVA), thins out and provides a lesser protection to the user, and may even provide a false sense of safety. In this study, the author employs the use of a dropped mass to evaluate the shock absorption capability of the mouthguard material. The author used two stainless steel balls as the dropped mass; one with a diameter of 1.0 inches, and another with a diameter of 2.0 inches dropped from 33.75 inches and 10.0 inches respectively. The dropped mass is made to impact a specimen resting on a force transducer which

records the impact. The peak force transmitted to the transducer is recorded, and carbon paper is inserted between the specimen and the transducer to estimate the contact area in order to calculate the transmitted impact stress. In addition to this data, a video camera is employed to capture the rebound height of the dropped mass, and calculate the energy dissipated by the specimen using an energy balance. The experiment is diagramed below (Figure 1, re-created from Park's figure).

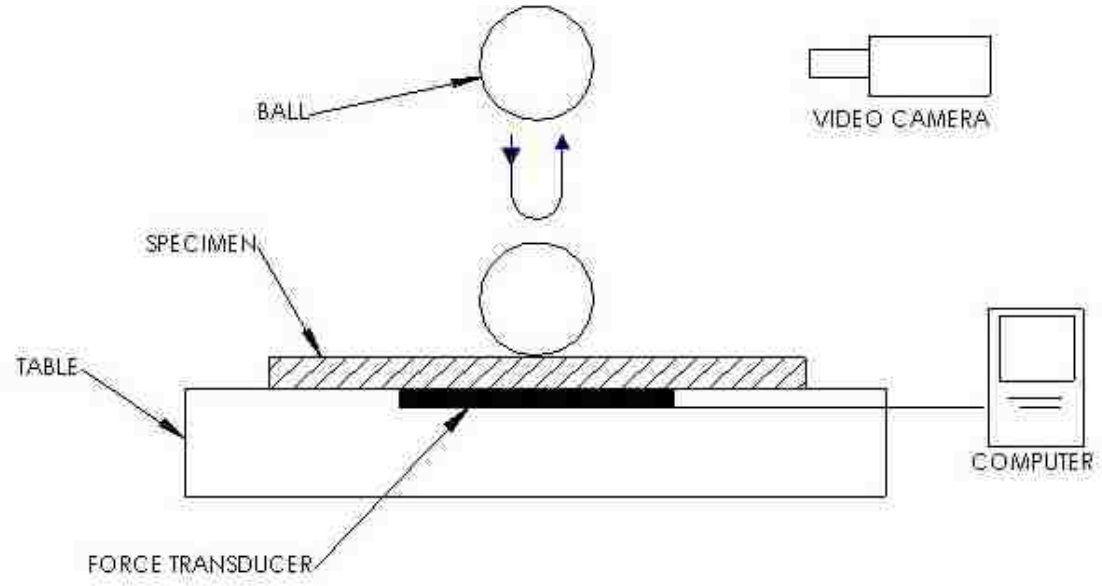

Figure 1 - Test set up used by Park

Park's testing was conducted on several thicknesses of EVA sheets (1, 1.5, 2, and 4 mm) and on sheets of 4 mm Pro-form™. As would be expected, the thicker sheets transmitted lower peak forces to the transducer. There are, however, no results published in this paper regarding the energy absorption. This may be a result of difficulty in determining the rebound height using a video recorder. Typical gaps between impacts

during a test would range in the order of milliseconds (this is gathered from testing presented later in this paper). If the video camera records at a rate of 30 frames per second (which is typical), then the camera only captures images of the event once every 33 milliseconds, and may miss the impact event entirely, making it impossible to gauge the rebound height of the dropped mass.

Bishop, Davies, and von Fraunhofer, 1985

In a study very similar to that of Park, several materials potentially used for mouthguards were tested. Bishop, Davies and von Fraunhofer chose to test nine mixtures of polyvinyl acetate (PVA) and polyethylene (Bishop, Davies, & von Fraunhofer, 1985). Among the properties tested were water absorption, compressibility, tear strength, static energy absorption, and of interest here, dynamic energy absorption. In this testing, dynamic energy absorption was measured using the method of energy balance where the initial height of a dropped mass is known and the rebound height is measured during the test. The energy absorbed is calculated using the following formula.

$$E_{absorbed} = mg(h_{initial} - h_{rebound})$$

For this test, a calibrated glass tube is placed over the specimen, and a 0.5" diameter steel ball is allowed to fall from a predetermined height within the tube onto the specimen. The rebound height is observed by means of a telescope. It is unclear how exactly the telescope was used to gauge the rebound height, but must be assumed that the height was estimated by eye. This could lead to error in the data due to the subjective measurement of the rebound height. The thicknesses of the specimen varied from 0.310

to 0.334 mm (7.7%), and as such, the energy absorbed by the material varied only slightly from 28.93 to 31.58 millijoules (9.2%). This result points to the importance of material thickness as it is related to energy absorption.

These first two studies focused on the raw material from which the mouthguards are made, and testing was conducted on material samples, or coupons, upon which a dropped mass is used to provide the impact and energy absorption is calculated using an energy balance. While this seems the most straight-forward method for determining energy absorption, many other metrics have been used to evaluate the performance of a particular mouthguard or material. Impact pendulums are used in a number of studies to provide the impact to the specimen, and finished mouthguards are used in a number of studies as the test specimen instead of material coupons. The metric used to evaluate the performance of a guard or material include integrating the force-time curve (solving for the change in momentum), or simply noting the reduction in the peak force transmitted to the mouthguard, or recording strain and acceleration of either the impacting body or the device to which the guard is attached. The studies presented next use a combination of these methods and show other ways to gauge the performance of mouthguards.

Darin R. Lunt et al, 2009

In this study, the researcher is examining the performance of different mouthguards under three specific environments where they are all conditioned for 1 hour at 37 degrees Celsius prior to testing (Lunt, et al., 2010). Ten samples of each type of mouthguard were conditioned in the following settings: dry (ambient), deionized water, and artificial saliva. Three types of mouthguard material were used for the samples,

namely: EVA, Pro-form™, and PolyShock™ of varying thickness ranging from 3.55 to 6.37 mm. The author normalized the results based on specimen thickness.

The specimens were impacted at 20 mph by a 0.5" diameter indenter containing a force transducer. The velocity of the impact object was provided by gravity in a drop-tower testing apparatus. The difference between this test method and that of the first two tests presented (which also used a dropped mass), is that the mouthguards were formed into a finished product prior to testing. This requires that the mouthguards be placed on a surrogate maxillary for the testing. The metric by which the samples are evaluated is provided by integrating the force-time curve of the impact (stated in the paper as the area under the force-time curve). The author makes an estimate of the total impact time for each of the types of mouthguards tested and sets the boundary conditions for the integration of the force-time curves based on this estimate. As in the studies previously presented, this estimation may lead to some subjective error in the results. The approach used during the study moves two steps closer than the previous studies to a real-life situation. The first step is the use of a finished mouthguard instead of representative coupons, and the second step is the inclusion of conditioning the mouthguards in an environment closer to in which they would be used. This approach does, however, introduce the possibility of unintended variation between samples of the same type due mainly to the process by which the mouthguards are formed wherein the material gets thinner in some places.

The following studies to be presented begin to explore the design of the mouthguard in more inventive ways. Where the previous three studies explored the

materials from which the guard is made, the basic design of the mouthguard remained unchanged, even if the specimen that were tested were unformed, the testing implied a single material guard. In the following studies, the researchers start to investigate the design, and modify the single-material guard to include features to either absorb the shock better (like air pockets or foam), or to distribute the shock better (like hard insertions or steel wire arches). Modifying the design of the guard may lead to the ability to provide a mouthguard that is thin enough to be tolerated and more comfortable by the user while still providing sufficient protection usually achieved by making the mouthguard thicker. This approach speaks to the heart of this thesis, and is presented here to show the work previously done in the field regarding the design of a mouthguard.

Westerman, Stringfellow and Eccleston, 2001

The goal of this study was to assess the impact performance of mouthguard materials with air inclusions (Westerman, Stringfellow, & Eccleston, 2002). The samples tested were all made of EVA, and had an overall thickness of 4 mm. The control group was a solid 4 mm thick EVA, and the experimental groups were EVA with three varieties of rectangular air pockets imbedded in the material. The first group had pockets that were 2 x 2 x 2 mm and 1 mm thick separating walls. The second group also had pockets that were 2 x 2 x 2 mm, but the separating walls were 2 mm thick. The third group had pockets that were 3 x 3 x 2 mm, and the separating walls were 1 mm thick. The experiment involved striking the samples with a flat, 20 mm diameter striker head using an impact pendulum machine. The impact here was equivalent to the energy of a cricket ball travelling at 27 mph (4.4 J). The investigators fitted the impact head with an

accelerometer and used $f = ma$ to determine the force transmitted to the mouthguard material.

The metric used in this study was the mean peak force transmitted through the mouthguard material as determined by the accelerometer. The results show a decrease in the peak force using all of the samples with air inclusions over the sample of solid EVA, with the best performer being the third group with the larger air inclusions giving a decrease of 32%. Although no attempt in this paper is made to calculate the energy absorption, the decrease in peak force is significant when varying the design to include the air pockets.

Takeda, 2006

The researcher in this study explores the use of a hard insert and space (air pocket) laminated between layers of EVA in the design of a mouthguard (Takeda, et al., 2006). The experiment employs a pendulum striker that impacts the mouthguard covering a specially designed device outfitted with strain gauges and an accelerometer. It is not stated in the paper what the maxillary surrogate is, but it appears to be tooth-shaped, and the design is shown below (Figure 2, re-created from Takeda's figure).

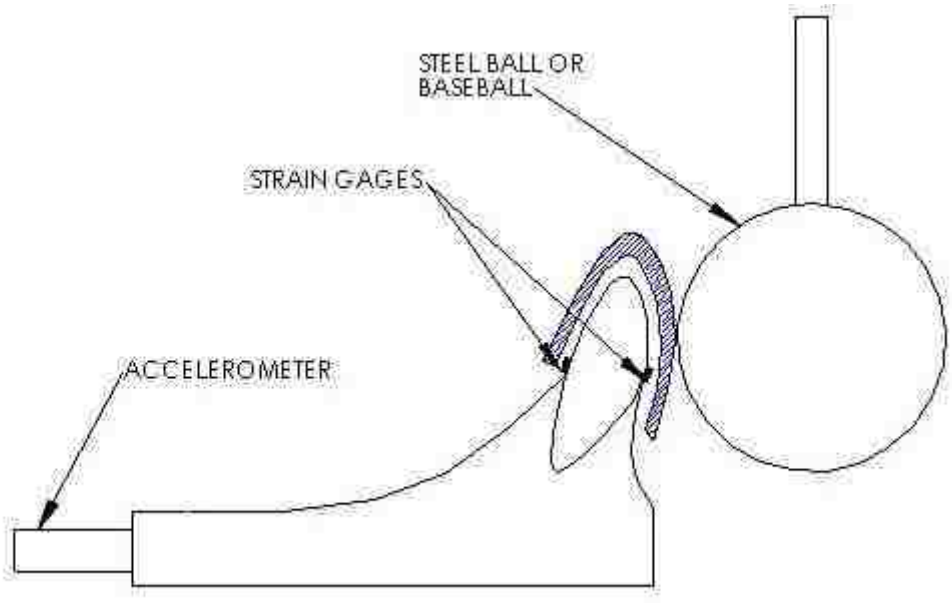

Figure 2 - Takeda testing apparatus

As indicated in the figure, this researcher used both a steel ball and a baseball as the impacting object and measured both distortion of the tooth and acceleration of the maxillary device. Three groups of mouthguards and a control (no mouthguard) were tested. A traditional EVA mouthguard, a laminated mouthguard with a hard acrylic resin inner layer, and another laminated mouthguard with a hard acrylic resin and a space between the resin layer and the tooth were the groups tested. All of the mouthguards tested were approximately 3.0 mm thick at the point of contact. For both measurements, acceleration and distortion, peak values during impact were used as the metric for performance. The results were presented as a percent reduction in either peak acceleration or distortion (strain) as compared to the control (no mouthguard). All mouthguards tested showed a significant reduction in acceleration and distortion with

both impact objects. With the steel ball, the EVA and EVA plus hard insert both showed acceleration reductions of 39.7% and 37.3% respectively with no statistical difference and the mouthguard with a hard insert and space showed a reduction of 49.3%. The distortion results showed a decrease in all cases with the EVA guard showing a reduction of 47.5%, the EVA plus insert 81.6% and the EVA plus insert and hard space showed a 98.3% reduction. Similar results when using the baseball as the impact object are reported although the reductions in acceleration are less pronounced and the reductions in distortion are almost identical.

The impact energy was not noted in this paper for either the case of the steel ball or the baseball, and at high impact energies, the buffer room given by the insert plus hard space might be depleted resulting in failure of this type of guard to protect the teeth to the degree reported in the study. The author contends that in higher energy impacts, the hard insert would break down and absorb much of the energy of the impact, but this is noted only anecdotally. It is also not noted what was used as the material for the maxillary surrogate or the exact construction of the model. Both would have significant effect on both the distortions and accelerations recorded during the impact of the tests.

De Wet, Dent, Heyns, and Pretorius, 1999

In this study, the author investigates five types of mouthguard designs by fitting an artificial skull with a variety of strain gauges and accelerometers and striking the skull mounted with the mouthguard (de Wet, Dent, Heyns, & Pretorius, 1999). A modal hammer outfitted with a load cell was used to record the force applied at the mouthguard, and strains and accelerations are measured. The modal hammer was attached to a

pendulum device to provide a repeatable impact for each of the tests. Like many previous studies, the control used is readings from the strain gauges and accelerometers with no mouthguard in place. The five types of mouthguards are as follows: 1 – a single layer of 2 mm Bioplast™ material, 2 – a 2 mm layer of Bioplast™ followed by a 3 mm layer of Pro-form™, 3 – a 2 mm layer of Bioplast™ followed by a preformed stainless steel arch and a second layer of 3 mm Bioplast™, 4 – a layer of 2 mm Bioplast™ followed by a piece of sponge and a second layer of 3 mm Bioplast™, and 5 – same as configuration 4 but the second layer of Bioplast™ was replaced with 3 mm Pro-form™. It is unclear exactly how this researcher interpreted the force values used in the analysis of the performance, but would appear as though the values presented are an average of the force over a given time interval. A sample output is shown below in Figure 3 (re-created from De Wet's paper).

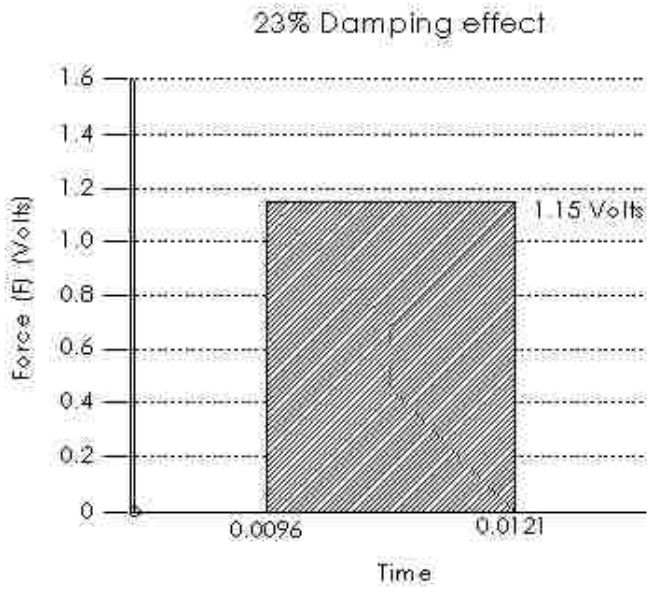

Figure 3 - Sample output of force value used in analysis

Note that in the output shown, no peak is displayed, but the time interval shown is 25 milliseconds which must represent the envelope of the entire impact event. Regardless of the exact metric used in this study, the results show what other studies have shown; that is, mouthguard usage reduces the shock to the maxillary. The best performing guard was type 5 which showed a 55% reduction in the 'force' transmitted to the artificial skull.

Discussion of Previous Studies

All of the studies presented in the previous sections show one thing unanimously; the use of a mouthguard reduces the energy transmitted to the maxillary during an impact. Regardless of the metric used, this was shown to be the case in all papers that were researched, including the ones presented here, and all others that were investigated. There are no international standards available for the testing of the shock absorption potential of mouthguard materials or designs (de Wet, Dent, Heyns, & Pretorius, 1999), so it is reasonable to expect the variations seen in the test methods presented. In addition to the variation in test methods, the metric by which the guards are evaluated also varies a fair amount. It is therefore reasonable to expect variations in the results obtained through the testing that has been done. What is shown to be consistently reported is the trend that thicker mouthguards provide better protection then thinner guards. Another trend that appears is that the use of an intermediate layer of either sponge or air aids in the shock absorption capabilities of the mouthguard.

Before continuing with further testing in this area, it is important evaluate the variety of test methods and metrics used in the previous testing. The methods used in the

testing fell into two main groups: the use of a dropped mass and the use of a modal hammer and pendulum. Both methods use gravity to provide the energy for the impact, but the dropped mass seems to avoid some complications that the pendulum may present. When using the pendulum approach, the modal hammer must be attached to the pendulum swing arm in some manner and the wire from the hammer must be attached to the device which records the data. This creates a few problems: first, the pendulum will surely have some undefined friction due to the motion of the swing arm relative to the housing, and second, the wire will have some degree of stiffness and will resist the motion of the swing arm. Both of these issues will add error into the experiment, and both are avoided when using the dropped mass approach.

Of the many metrics for performance that were presented, the use of an energy balance to calculate energy absorption seems to be the most straight-forward and makes the most sense as a scientific measure of the energy absorbed by the mouthguard. While this may not be the most clinically relevant, it makes the most sense to use as a practical measure. The problem with this metric lies not in the metric itself, but with the means by which the measurement is taken. In the first two studies, this metric of performance is used, and in both cases the energy balance is calculated using rebound height of a dropped mass. The rebound height, as previously mentioned, must be estimated and would certainly lead to experimental error. In the first study, a video camera (of unknown specifications) is used to capture the rebound height during the experiment. This method leads to problems due to the frame rate limitations with most video cameras as discussed before. A solution to this problem might be to use a high-speed camera to capture the rebound height of the dropped mass. Although the use of a high-speed

camera solves the frame rate issue, the actual measurement of the rebound height would necessarily made by eye, and with all practical measures assumed to be taken, the resolution would most likely be no better than 1 or 2 mm. While the accuracy of this method would surely be better than using a standard video camera, the data would still be subjective and prone to some error. In the second study presented (that of Bishop, Davies, and von Fraunhofer), the issues of measuring rebound height are the same and compounded by the fact that no recording equipment is used. The study mentioned using a telescope to measure the rebound height, but it can only be assumed that the measurement was taken real-time.

It is concluded that while the use of an energy balance would be an ideal metric for determining the energy absorption of a possible mouthguard, the practical obstacles prove to be somewhat substantial. As a result this metric has not been chosen for use in the testing that was conducted and presented in this paper. Which leaves the other metrics used; namely, peak force values (or peak acceleration values) and peak strain values. Peak force values, or more broadly, the force versus time plots are useful in gauging the performance of the mouthguard; it is difficult to relate these to energy absorption. In one study (Lunt, 2009), the author uses the area under the force-time curve as a measure of energy absorption, however this not a measure of energy but rather a measure of momentum change imparted to the impacting object as given by the following equation.

$$\Delta p = \int_{t1}^{t2} F dt$$

Beyond the peak force derived from the force-time curve, the width of the curve (time of contact) could be used as a measure of performance. For a given energy, the peak force is reduced as the time of contact increases, so larger contact times would indicate better performance. This is also a difficult measurement to take, because the exact point where the impacting object makes contact and then rebounds off of the surface of the mouthguard is difficult to tell from a force-time curve. It may be possible to take the time at which force value exceeds some pre-set nominal value as the threshold defining the contact time, and use this as a gauge.

For the testing that will be presented in this study, the peak force transmitted through the mouthguard will be used as one metric of performance. In addition an energy balance will be used as a second metric, but the means at which the energy balance is obtained will be quite different from any of the ones previously discussed. Detailed in Chapter 4, it is hoped that this new method will prove superior to the ones presented in this chapter.

Overview of Design and Testing

What follows in the next few chapters is a description of tests performed on a novel mouthguard design that include similar features to some of the mouthguards presented earlier. It is clear that improvements can be made in arena of performance (in terms of shock absorption) by altering the design of the traditional, one-material mouthguard to include layers with varying mechanical properties. It is the goal of this research to test a mouthguard design that incorporates a hard layer (Nitinol insert) and a soft foam layer, and determine whether the combination provides better shock absorption

capabilities than that of the individual parts alone. The use of a hard insert was proposed by de Wet, Heyns, and Pretorius in the form of a stainless steel arch, with the idea being that it would distribute the force of an impact.

"... if the mouthguard is soft and the force is distributed through a steel arch, the force will be spread over a number of teeth."

Their testing showed some reduction (7%) in the registered force transmitted to their artificial skull model over a design that was similar only lacking the steel arch. They were not the only ones to suggest the use of a hard layer of material to distribute forces. Takeda proposed, and tested, a similar idea using a hard acrylic layer with a space separating this layer from the traditional mouthguard material (Takeda, et al., 2006). Again, his testing showed increased protection using this approach.

In addition to the use of a hard insert layer, the use of a soft intermediate layer has been explored and shown to be effective in reducing the shock of an impact. Air cells like the ones used by Westerman have been effective (Westerman, Stringfellow, & Eccleston, 2002), and a soft sponge layer have also been effective (Buslara, 1998). The use of a soft layer, then, seems an obvious choice to include in the design of a new mouthguard.

The combination of both a hard insert and a soft layer should prove to be a superior design than the use of either component alone, and has been chosen for the design to be tested. In addition to testing this design with EVA, Nitinol and foam, samples including only foam and only Nitinol with no insert will be tested and used to compare contributions from each component.

The testing will be divided into two tests, both of which will be conducted with the use of a drop-weight tower apparatus. For both tests an impact head will be attached to the crosshead of the drop tower and used to provide the impact to the test samples. In addition, both tests will involve recording the force-time curves transmitted through the sample by using a load cell. In the first test, the sample will rest on a flat plate, and only the force-time curve will be used to evaluate the performance of the sample. This test is detailed in chapter three. In the second test, the sample will rest on a simply supported beam outfitted with a strain gauge. The other aspects of the test will remain the same, including the use of a load cell to register the force transmitted through the sample and the beam. In this test, the force-time curve and the strain values in the beam will be used to evaluate the performance of the sample by calculating energy absoption. This test is detailed in chapter four.

CHAPTER 2

SAMPLE PREPERATION

Samples of several mouthguard configurations were manufactured into flat coupons that represent the mouthguard designs instead of fully formed mouthguards. This approach has been used in several studies, and is seen as the simplest and most reliable method for testing the mouthguard designs. Many studies have been performed using fully formed mouthguards, but the problem with this approach is the thinning that occurs during the forming process. It was decided to avoid the variability of thinning and the added geometric complications by simply using flat, rectangular coupons to represent the different mouthguard configurations. What follows in the next few sections are descriptions of the materials used, and reasons for their use. After that, the sample construction is detailed.

EVA layers

Ethylene Vinyl Acetate (EVA) was chosen for the design for many reasons including ease of use, availability and familiarity within the dental community. EVA is used commonly for the production of off-the-shelf boil-and-bite mouthguards as well as custom mouthguards, so it presents itself as an obvious choice for use in the novel mouthguard designs tested and presented in this paper. The choice to test 1 mm and 2 mm layers was made based on testing that shows little increase in protection for mouthguards measuring more than 4 mm (Westerman, Stringfellow, & Eccleston, 2002). For the designs tested here, the overall thickness will range from 2 mm to 4 mm in the

control group (inner plus outer EVA layers), and slightly thicker for configurations with Nitinol and/or foam inserts.

Nitinol

The nickel titanium alloy (Nitinol) insert used in this study is intended to distribute the force of an impact over a larger area then the EVA layer alone would do. This is an approach suggested by several researchers, whether by using a hard insert as was suggested and tested by Takeda or by using a stainless steel arch as was used by de Wet, Heyns, and Pretorius. There are some distinct advantages afforded by the use of Nitinol over a stainless steel wire arch. The first advantage is the extraordinary ability that Nitinol has to undergo large elastic deformations without permanent deformation. Clinically, this would allow the user of the mouthguard to deform it without the risk of permanent damage, for instance when removing the guard and wedging it in a helmet or face protector, or even inadvertently stepping on the guard. Another advantage to the material is the ability to form it into a curved shape that would match the curvature of a typical maxillary via a heat treatment process.

The Nitinol inserts used in this study are thin sheets that measure 9 mm wide by 48 mm long and 0.33 mm thick. The raw material for these inserts was purchased from Memry GmbH (Germany), and is alloy S (superelastic) flat, annealed oxide free. The raw material was supplied as a sheet 103 by 455 mm and 0.33 mm thick, and was sent to Directed Light Inc. (San Jose, CA) to be laser-cut into the shapes used in the coupons. The length and width were chosen to cover the central and lateral incisors of the maxillary as these are the most commonly damaged teeth during sports activities

(Andrade et al. 2010). Three variations of the Nitinol inserts were laser cut by the supplier; the first was simply a rectangular strip 9 by 48 mm with no other features, the second had the same 9 by 48 mm footprint and featured 73 circular holes 1.5 mm in diameter and evenly spaced through the footprint, and the third featured 121 holes also 1.5 mm in diameter and evenly spaced. Figure 4 shows an example of the Nitinol inserts as they arrived from the laser cutter.

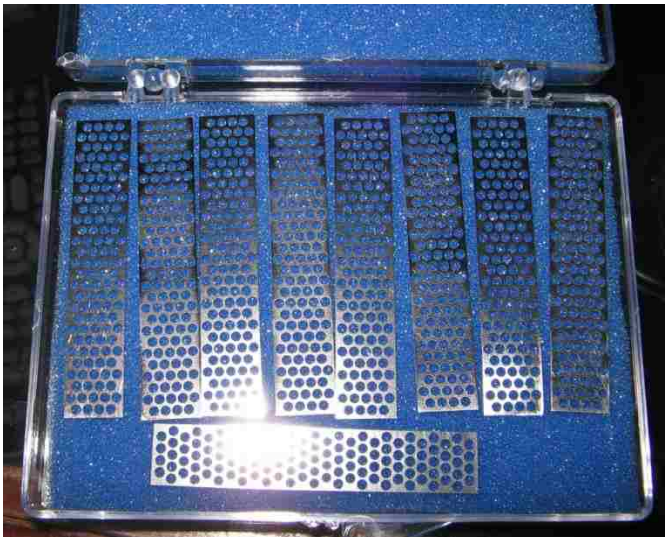

Figure 4 - As-cut Nitinol inserts

The three styles of inserts created can be identified by the amount of void space each contains due to the holes present. This void space can be defined as a porous area fraction (PAF), which is the void area divided by the footprint area, and is calculated as follows:

$$PAF = \frac{n\pi D^2}{4A}$$

where D is the diameter of the holes, n is the number of holes, and A is the area of the footprint. The three styles of inserts have 0%, 31%, and 50% PAF, and are labeled in this manner throughout the testing results. The purpose of the holes is two-fold. It allows the insert to be tailored to a certain stiffness and it provides a means to mechanically anchor the insert to the EVA layer(s). The actual design drawings are shown in appendix A. Although not done in this study, one could vary the arrangement of the holes (or whatever kind of void) to vary the stiffness across the area of the insert. The choice of patterns in these inserts is somewhat arbitrary, because at the time they were created, no data regarding how they would behave was available.

One disadvantage to the use of Nitinol is the difficulty in machining as compared to other materials (like stainless steel) using conventional machining methods. Laser-cutting and electric discharge machining (EDM) are the most common methods for machining the material and both can be very expensive. The other real disadvantage to Nitinol is its own expense as a raw material. It is for this reason that a limited number of Nitinol inserts were manufactured. From the original sheet provided by Memry, only 27 inserts were manufactured (9 of each style).

Foam

The choice to use foam as one of the layers in the mouthguard was the ability of foam to absorb impact energy in the form of strain energy by compression. Any number of foam materials can serve this purpose. Several foam materials were investigated for

use ranging from open and closed cell polyurethane to natural rubber foams. The foams investigated all came in raw sheet form or roughly 12.7 mm thick and 150 mm square from McMaster-Carr. Several attempts were made to cut the foam into repeatable accurate strips suitable for the coupons used in testing, but it proved too difficult to produce such strips, and this method was abandoned. What proved to be much more effective was to use foam tape that was provided in 12.7 mm strips that measured 0.79 mm thick (also from McMaster-Carr), and cutting these to the final width and length using a box-cutter and the Nitinol inserts as a guide. The tape is PVC foam with a thin acrylic adhesive on both sides, McMaster-Carr part number 76545A85.

Coupon Configurations

The coupons were designed to be 25 mm wide and 60 mm long. All of the test coupons incorporated an inner and outer layer of EVA with varying materials laminated between these inner and outer layers. Four basic configurations were tested, and are listed below.

Configuration 1: outer and inner EVA layer laminated together.
Configuration 2: outer and inner EVA layer with a Nitinol insert.
Configuration 3: outer and inner EVA layer with foam.
Configuration 4: outer and inner EVA layer with a Nitinol and foam insert.

Within each of these four basic configurations, variations to the EVA thickness were made. In all cases, the inner and outer layer was either 1 mm thick or 2 mm thick giving rise to 3 variants of a given configuration: 1 mm inner and 1 mm outer, 1 mm

inner and 2 mm outer, 2 mm inner and 2 mm outer. In addition to variations of the EVA layers, the Nitinol layer also varies in its design. In configuration 2 and 4, three designs of Nitinol insert were used as were described in the section on the Nitinol insert. In all, 24 different designs were tested and listed in Figure **5**.

Configuration 1				
Design #	Inner EVA	Outer EVA	Nitinol PAF	Foam
1	1 mm	1 mm	-	-
2	2 mm	1 mm	-	-
3	2 mm	2 mm	-	-

Configuration 2				
Design #	Inner EVA	Outer EVA	Nitinol PAF	Foam
4	1 mm	1 mm	0%	-
5	2 mm	1 mm	0%	-
6	2 mm	2 mm	0%	-
7	1 mm	1 mm	31%	-
8	2 mm	1 mm	31%	-
9	2 mm	2 mm	31%	-
10	1 mm	1 mm	50%	-
11	2 mm	1 mm	50%	-
12	2 mm	2 mm	50%	-

Configuration 3				
Design #	Inner EVA	Outer EVA	Nitinol PAF	Foam
13	1 mm	1 mm	-	.79 mm
14	2 mm	1 mm	-	.79 mm
15	2 mm	2 mm	-	.79 mm

Configuration 4				
Design #	Inner EVA	Outer EVA	Nitinol PAF	Foam
16	1 mm	1 mm	0%	.79 mm
17	2 mm	1 mm	0%	.79 mm
18	2 mm	2 mm	0%	.79 mm
19	1 mm	1 mm	31%	.79 mm
20	2 mm	1 mm	31%	.79 mm
21	2 mm	2 mm	31%	.79 mm
22	1 mm	1 mm	50%	.79 mm
23	2 mm	1 mm	50%	.79 mm
24	2 mm	2 mm	50%	.79 mm

Figure 5 - Mouthguard configurations

Coupon Construction

The mouthguard coupons were manufactured at the Shadow Lane campus of UNLV (School of Dental Medicine) with the help of dental students using their laboratory. The method for construction followed very closely the method for constructing any type of custom mouthguard. The machine used for forming the mouthguards was a Ministar™ pressure forming machine (Great Lakes Orthodontics; Tonawanda, NY) shown below (Figure 6). Used in the traditional manner to make

mouthguards, the machine works by heating a layer of EVA and then applying pressure to form the EVA over a model of the patient's maxillary. Each type of material used in the machine has manufacturer recommendations for heating and cooling times which depend on the material properties and thickness. For our use in creating mouthguard coupons, a maxillary model was not used, and instead, the outer EVA layer was heated and then pressurized over whichever insert was needed for the particular configuration (i.e. Nitinol insert, foam, or none in the control), and laminated to the inner EVA layer. Manufacturer specifications were followed for heating and cooling times.

Figure 6 - Ministar™ forming machine

Some problems were encountered during the process of laminating the layers together including some adhesion issues between the inner and outer layers of EVA and air pockets being formed between the outer EVA layer and the Nitinol layer. The latter issue was solved by puncturing the inner EVA layer with two small holes towards the ends of the coupons as not to interfere with testing that would impact the center of the

coupons. Each layer of inner and outer EVA was formed over three inserts in order to maximize the use of the EVA material. A sample of the product from the forming machine is shown below (Figure 7).

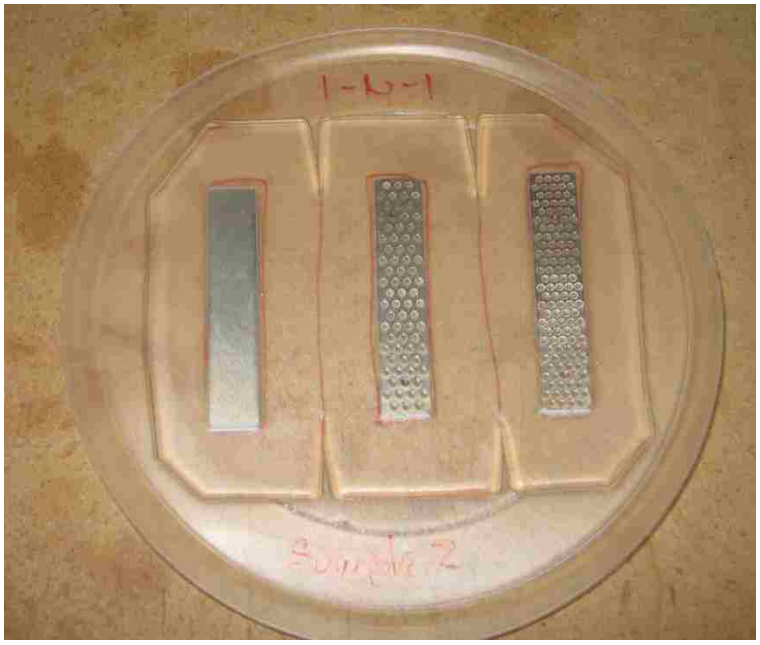

Figure 7 - Coupons from forming machine

Once the layers were laminated together, the coupons are cut to their final dimensions using a box cutter. Special care was taken to control the width of the coupons, and the length of the coupons was controlled to a lesser degree. The reason for this is that the amount of material that gets compressed during the testing is a function of the width and the thickness and not the length. This will become clear in the following chapters on testing. The process of cutting the coupons to final size is illustrated below

(Figure 8), where the coupons are cut to width (center) and then trimmed to final dimensions (right).

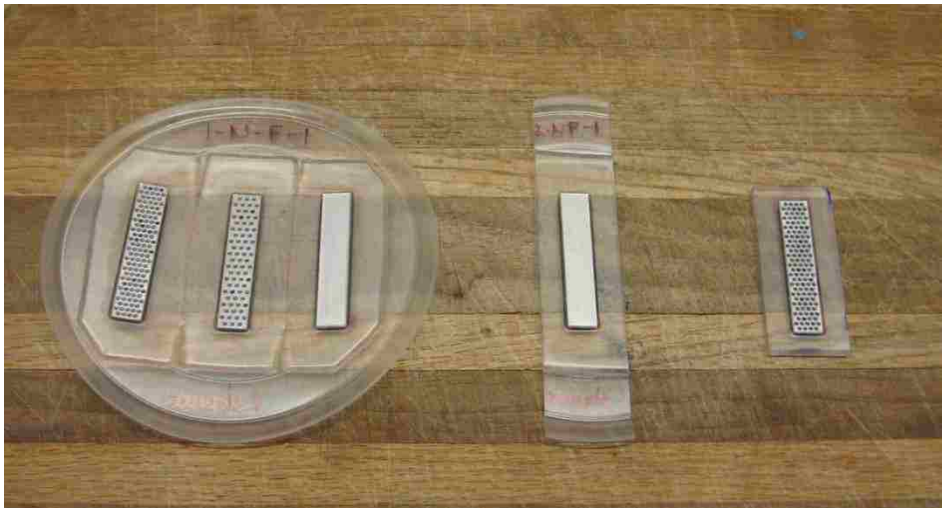

Figure 8 - Coupon sizing process

At this point, each test coupon is individually bagged and labeled indicating the construction. The labeling method indicates the thickness of the inner and outer layers of EVA, and the presence of a Nitinol layer and/or foam layer. The PAF of the Nitinol is also indicated. A sample of the labeling method is 1-N-F-1 50, which would indicate a 1mm outer EVA layer, a 50% PAF Nitinol layer, a foam layer and a 1mm inner EVA layer.

Due to the limited number of Nitinol inserts that were produced, these inserts had to be reused in order to produce the number of coupons desired for the testing. The inserts were removed with box cutters, and cleaned using acetone (if required). The

cleaning was needed to remove residual foam and adhesive in the case of coupons that had an intermediate foam layer. No changes were made to the construction process while using the recycled inserts. No damage was observed in any of the samples removed either from the testing or the removal process except in the case of some of the 50% PAF inserts. In some instances, the insert was removed, and it appeared to have broken during testing. It is assumed that it broke during the testing because the break was near the impact area in the coupon. This is discussed further in Chapter 5 in the section on sources of error.

CHAPTER 3

FLAT PLATE TESTING

The simplest method for testing the shock absorbing capability of a given mouthguard configuration involves the use of a dropped mass. This method has been used by several researchers, and as discussed at the end of chapter 1, it presents a simple and effective method for testing. The idea is to place the test coupon on a flat surface and drop a mass (under the influence of gravity) striking the coupon. The plate is attached to a load cell which records the force transmitted to the plate via the coupon. The exact experiment is described in the next section.

Experiment Design

An instrumented drop-weight impact tower is employed to provide and control the dropped mass. The machine consists of a crosshead guided by two polished steel rods, a base to which a load cell is attached, and a control system which moves the crosshead to its initial drop height. Several interchangeable plates may be attached to the crosshead to adjust the mass for the desired experiment. The machine is an Instron™ Dynatup drop weight impact tester (Norwood, MA) model 8250. For this testing, 2.27 kg (5 lb) plates were attached to the crosshead, and the impact object is a 51 mm (2.0”) diameter machined aluminum 6061 cylinder with a thickness of 38 mm (1.5”). The impact object is bolted to the crosshead and plate assembly via ½-13 bolt. Bolted to the base of the machine is a model 200M70 ICP® force sensor made by PCB Piezotronics (Depew, NY) with a 22.24 kN load capacity. Two flat, aluminum 6061 plates are bolted together and, in-turn, bolted to the load cell. Technical drawings of the flat plates are

given in appendix B. It would be simpler to use a single flat plate, but this would leave a counter bore hole in the center of the plate (to accept the bolt attaching the plate to the load cell). This hole would lie directly beneath the test coupon at the point which the impact object would make contact with the coupon, and may interfere with the results. To overcome this, two plates were bolted together to provide a smooth surface for the test coupon to rest on. The arrangement of the crosshead with impact object and flat plates bolted to the load cell is shown below (Figure 9).

Figure 9 - Flat plate and hard impact head in drop tower

The total mass of the crosshead, plates, impact object and hardware is 2.75 kg. The initial height of the impact object for testing was set at 50.8 mm (2.0") providing a potential energy of 1.37 Joules (calculated from $E_p = mgh$, and neglecting any losses

due to friction or other sources). The drop height is set using a gauge block and the machine is set to return to this height by means of a hall-effect sensor (this is the L-shaped bracket to the right of the crosshead in Figure 9). The sensor was positioned by allowing to machine to return to its automated return position (controlled by the sensor), and adjusted until the gauge block just slipped between the flat plate and the impact object. The drop height (and potential energy) is therefore a conservative estimate, and does introduce some error into the experiment. It is for this reason, tear-down and set-up of the machine were limited as much as possible.

For each test, the test coupon is adhered to the flat plate using transparent double-sided tape (Scotch® Permanent Double Sided Tape). While this adds an additional component, and possibly an additional shock absorbing material to the testing, it is very thin and neglected as a contributor to the shock absorbing capability of the test coupon. Furthermore, this tape is used in all of the testing, and whatever effect it may have on the results, the effect would be consistent for all coupon designs. The coupons are positioned in the center of the plate lengthwise from left to right (as viewed from the front of the machine). At the point of contact, the arrangement of the impact object, coupon and plate is shown below (Figure 10).

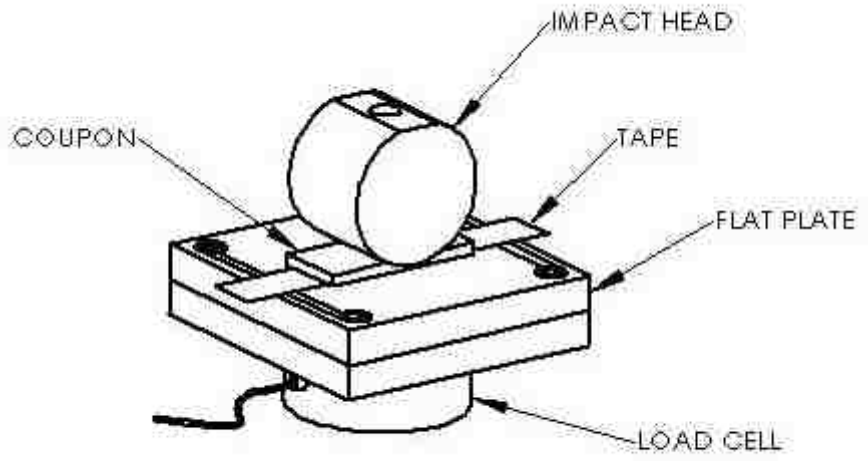

Figure 10 - Component arrangement at impact (to scale)

The signal from the load cell is passed through a signal conditioner (ICP Sensor Signal Conditioner, model 482 A21) and into an oscilloscope (Yokagawa DL750 ScopeCorder, model 701210) for viewing and recording. The oscilloscope was set to record the signal at 1MS/sec (1 million samples per second), and set to trigger recording 20% of total time (2 ms) prior to the point of impact as signaled by the load cell. A total of 10 milliseconds worth of data was recorded for each test. The signal recoded by the oscilloscope is in millivolts and is processed in Microsoft Excel (2010 Student version) by converting the signal to pounds-force using the conversion of 1.0 mV/lbf as provided by the load cell data sheet (PCB Piezotronics, 2005). A sample of a test after processing in Excel is shown below (Figure 11). 10 tests were conducted for each configuration, and a new sample of any given configuration was constructed for each test.

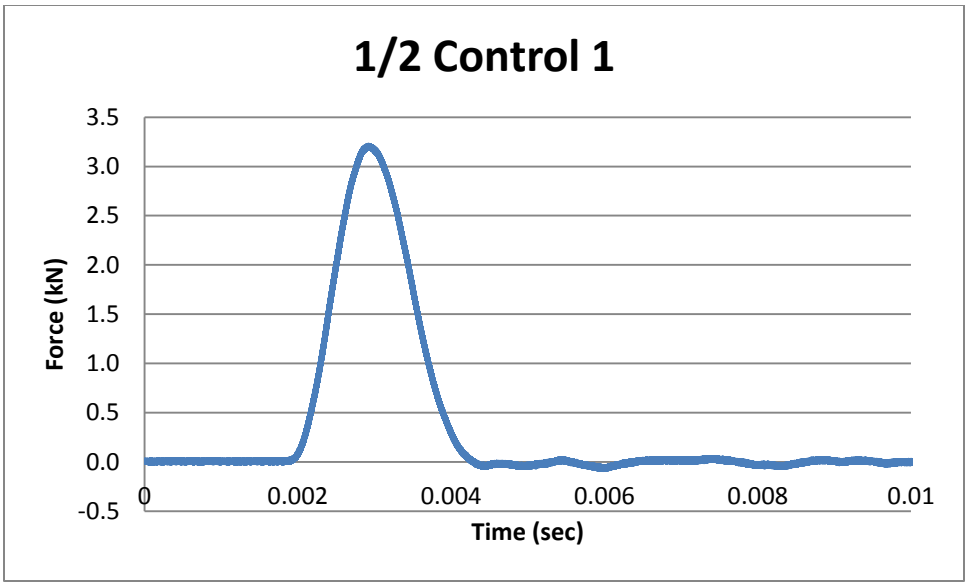

Figure 11 - Sample of test data after processing

Results

The data from all of the testing was compiled in Excel, and the performance of each configuration was compared to the control group. The data from the ten tests for each configuration were averaged and used for comparison. The results for all three groups are shown in the next three figures. The plots show the average value of peak force for the ten tests in each configuration along with the standard error represented by the error bars.

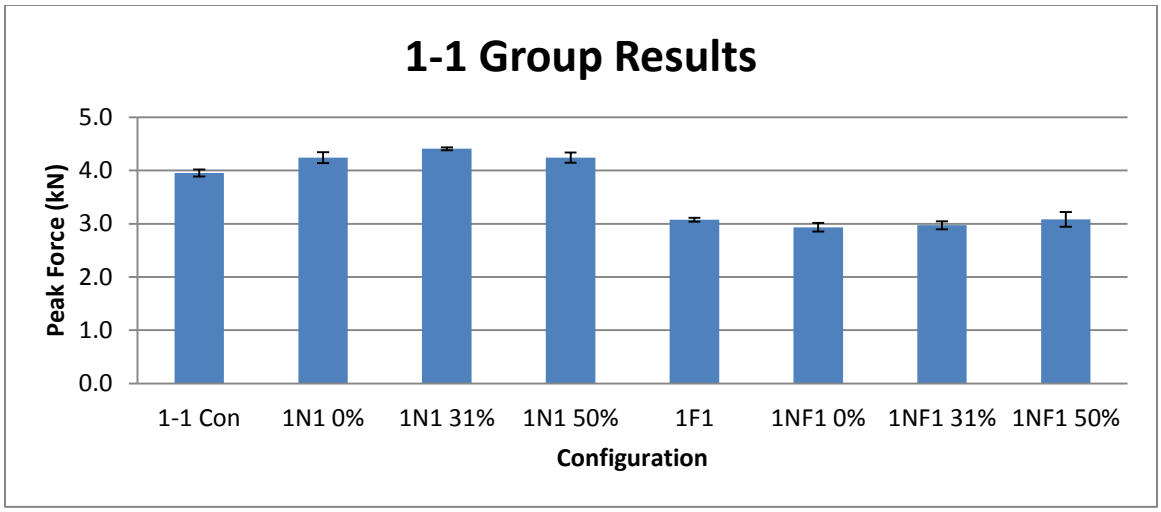

Figure 12 - 1-1 Group results

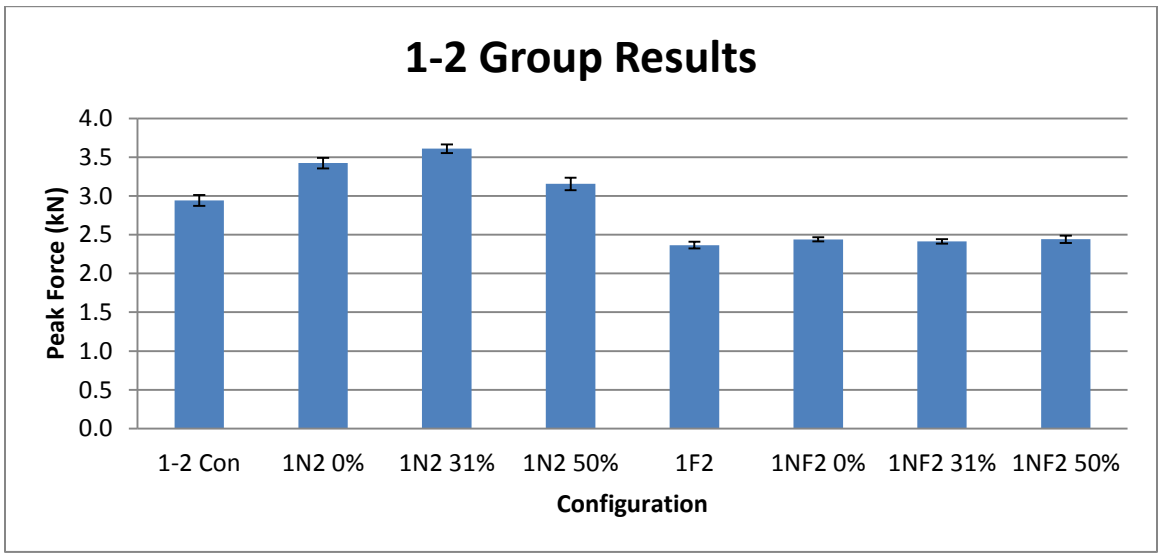

Figure 13 - 1-2 Group results

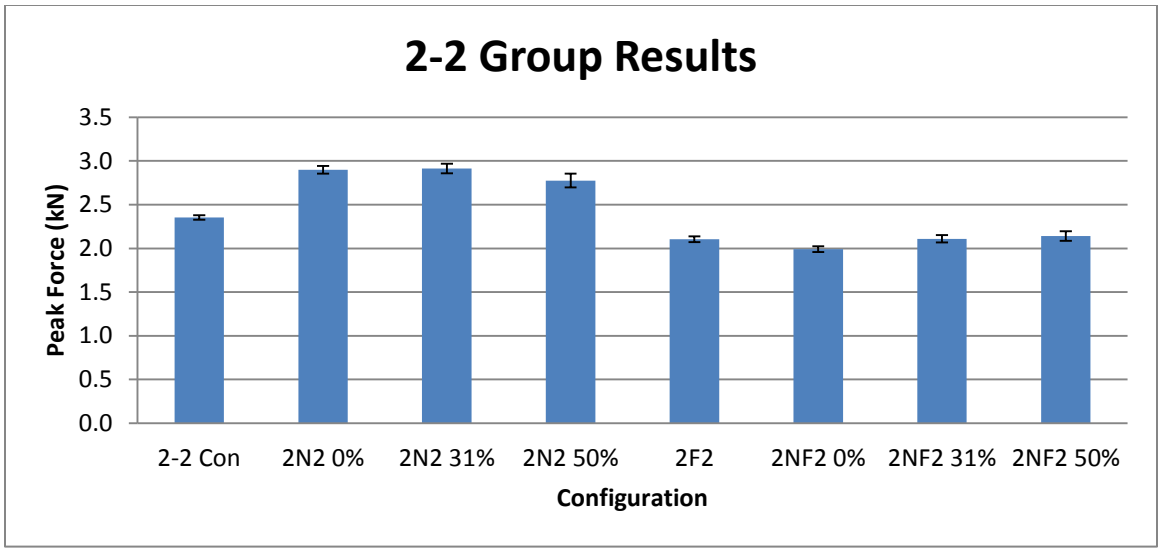

Figure 14 - 2-2 Group results

In order to gain a better idea of what the results mean, the data must be normalized in some manner to the thickness of the sample, because as mentioned before, the thickness of the sample greatly affects the ability to absorb the shock of impact. To do this, the average value of transmitted peak force and average thickness were calculated for the three control groups (1-1, 1-2 and 2-2 groups). The average peak force and thicknesses were then calculated for each of the other configurations. To compare the novel configurations to the control, several steps were taken; the first was to calculate the decrease in peak force as compared to the control, the second was to calculate the increase in thickness as compared to the control, and finally, the decrease in peak force was divided by the increase in thickness giving the following gauge for performance.

$$Performance\ Index = \frac{\%\ decrease\ in\ force}{\%\ increase\ in\ thickness}$$

The comparison in performance to the control was made in three categories and the configurations were separated according to the thickness of the EVA inner and outer layers, so that a configuration with 1 mm inner and 2 mm outer EVA layers would be compared to the 1-2 control group, and the same was done with the configurations having 1mm inner and outer EVA layers and 2 mm inner and outer EVA layers. The novel configurations are all thicker than their associated EVA only control group, so an adjustment was made in order to compare the performance of a given novel configuration to an EVA only control group of the same thickness. This was done by plotting the average peak force versus thickness for the three EVA only controls, and fitting a curve to this data in order to predict how an EVA only sample of any given thickness would perform. The plot is shown below (Figure 15).

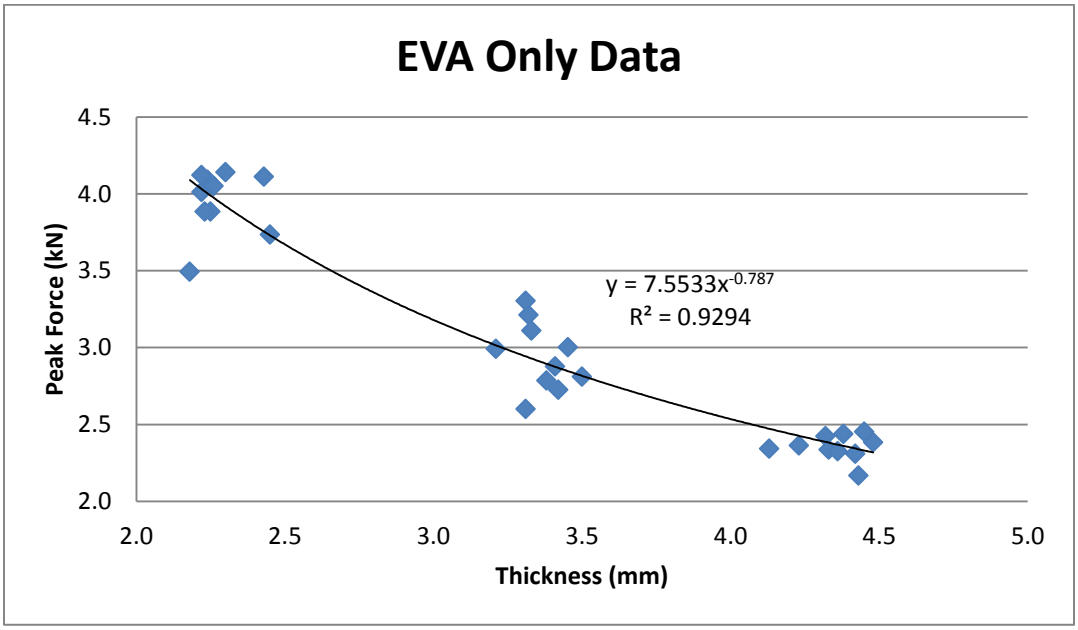

Figure 15 - Curve fit to control group

Using the equation of the curve fit provided by the data above, the performance of each novel configuration can be compared to an EVA only sample of a *would-be* same thickness. The results of this comparison are shown in the next three figures (Figure 16 through Figure 18).

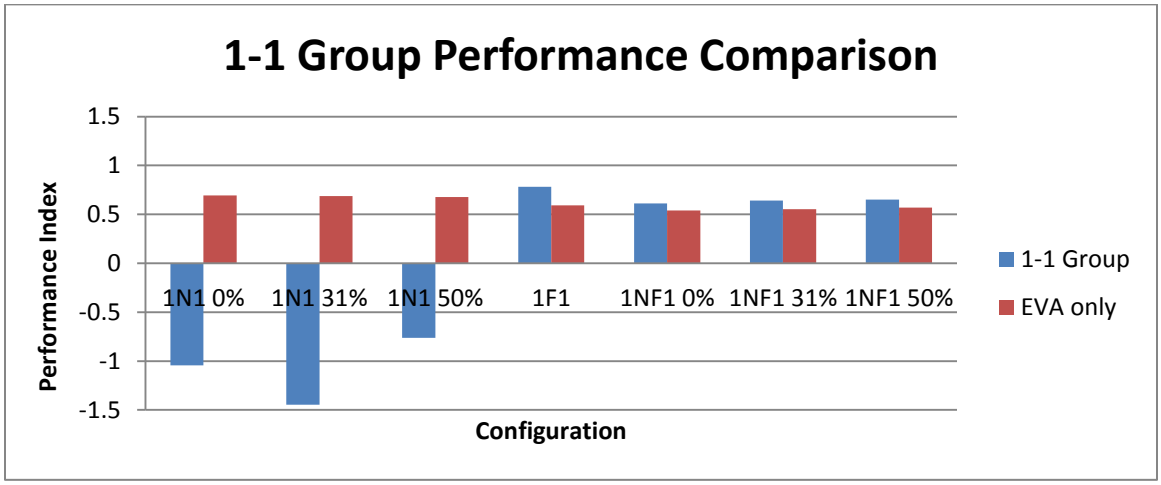

Figure 16 - 1-1 Group comparison

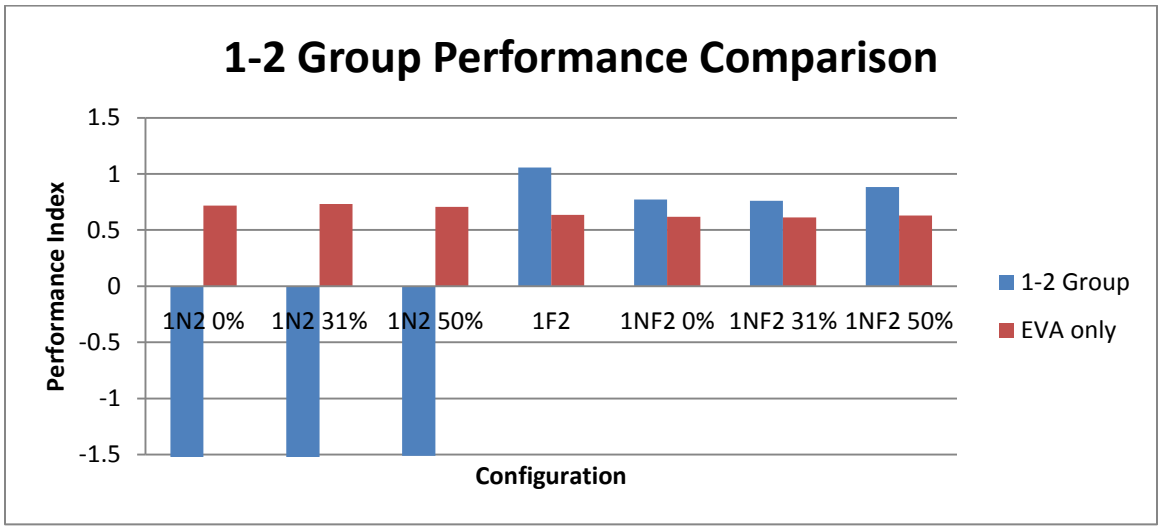

Figure 17 - 1-2 Group comparison

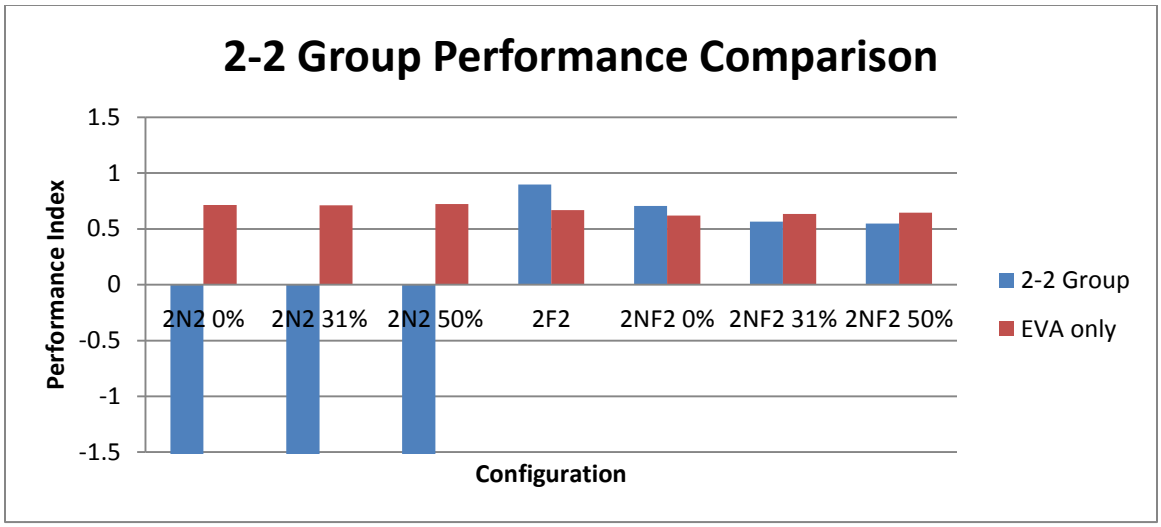

Figure 18 - 2-2 Group comparison

What becomes immediately evident in the plots is the poor (relative) performance of the EVA/Nitinol/EVA group. The plots show that an EVA only sample of the same thickness as that of the sample containing the Nitinol would actually perform better, and that the inclusion of the Nitinol is a detriment when tested by this means. The other trend that appears is the small increase in performance for the experimental groups that include a foam layer. These trends can be seen in relation to the control groups in the graph below (Figure 19).

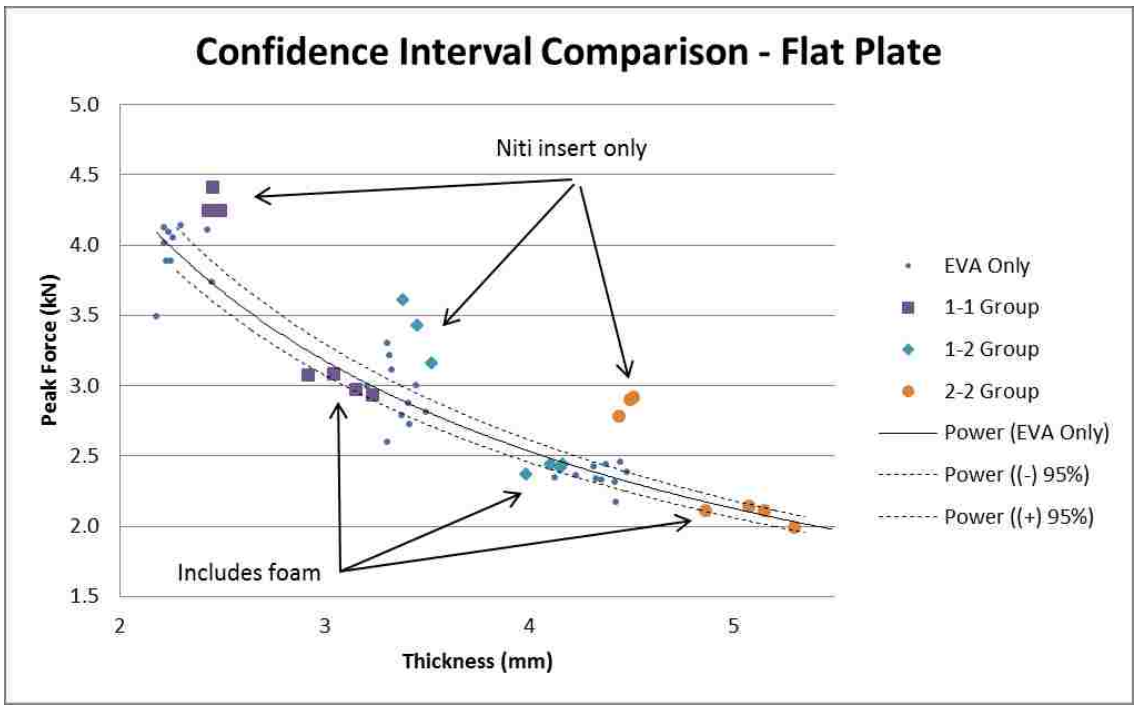

Figure 19 - Confidence interval comparison

The central curve fit in this graph (solid line) is generated from the control group data for all thicknesses. The 95% confidence interval lines (dashed) are generated by calculating the 95% confidence intervals for each control group using the following formula (Ehrenberg, 1982).

$$C = \mu \pm z^* \frac{s}{\sqrt{n}}$$

Where μ is the sample mean, z^* is 1.96 (for 95% confidence level), s is the standard deviation, and n is the sample size (10). The confidence interval lines were created via curve fit (power to match the curve for the entire data set), and extended by one unit to envelope the thicker samples.

The graph confirms what has been shown in the previous analyses, which is that the novel designs with a Nitinol insert only perform poorly in relation to the controls, and that the designs including a foam layer perform only marginally better, and that there is a good chance that there is no real difference between these designs and the control.

In the next chapter, another test design is used to evaluate the performance of the mouthguard coupons. Modifications are made to the fixture to include a simply supported beam, and the samples are tested again. The experimentation follows closely what has been described in this chapter, and is detailed in the next.

CHAPTER 4

SIMPLY SUPPORTED BEAM TESTING

While the previous testing gives a good indication of the performance of the novel mouthguard design (and its constituent parts), the coupon is not allowed to deflect, and the stiffness of the device may not enter into the results. Essentially what is tested is the ability of the sample to absorb and distribute force via compression. That is, there is no deflection of the bottom surface of the mouthguard coupon. And while there is no attempt made in this testing to replicate the maxillary either geometrically or materialistically, by disallowing deflection, one mode of energy dissipation is being left out. That is, the ability of the mouthguard to dissipate energy through deflection is ignored.

Experiment Design

In this test, the mouthguard coupon is placed on a simply supported beam, allowing for deflection of the coupon and beam. To be clear, no attempt is made here to replicate the maxillary in any way, but rather, to allow this additional mode of energy dissipation during the test. The simply supported beam is a 102 mm long by 51 mm wide, 6.35 mm thick (4” x 2” x 0.25”) aluminum 6061 precision ground blank purchased from McMaster-Carr in finished form and machined to length. The beam is supported by two ground steel dowel pins, each 51 mm long with a 6.35 mm diameter (2” x .25” dia). The two dowel pins are mounted (and glued) to the top surface of the flat plate used in the previous test which is modified with two grooves spaced 89 mm apart (3.5”) to accept the pins. The beam sitting on the pins and flat plate is shown below (Figure 20). Other

than the two grooves that are machined into the flat plate, no other modifications to the fixture were made.

Figure 20 - Beam on flat plate

A strain gage was bonded to the lower surface of the beam centered in both length and width (Vishay, model CEA-06-240UZ-120). The strain gage was oriented longitudinally to measure strain along the length of the lower surface of the beam, and the sensitive portions of the gage were covered with blue painter's tape to protect the gage during testing and isolate the electrical leads from the plate as shown below (Figure 21).

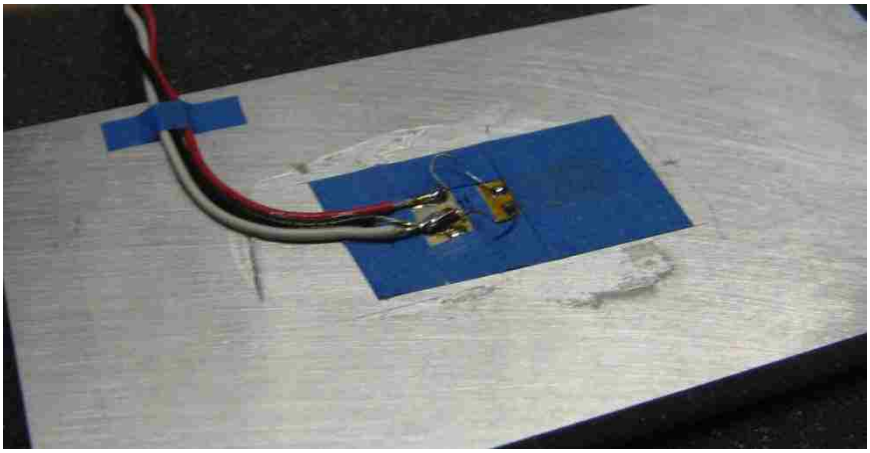

Figure 21 - Strain gage attached to beam

The addition of the beam and the strain gage allows for the simultaneous collection of force-time data and strain-time data. The strain data is collected via the same oscilloscope as is the force data. The signal from the strain gage is sent through a signal conditioning amplifier (Vishay, model 2310A) before reaching the oscilloscope. In order to convert the voltage output from the signal conditioning amplifier, the following equation is used, as provided by equation 7 of the user's manual for the amplifier box (Vishay Micro-Measurements, 2004).

$$V_{out} = 10^6 V_{br} A \frac{K}{4} \mu\varepsilon$$

where V_{out} is the voltage into the oscilloscope which gets recorded during each test. V_{br} is the excitation voltage of the gage circuit, A is the amplification, K is the gage factor of the strain gage, and $\mu\varepsilon$ is the microstrain experienced by the gage during the test. This equation can be rearranged to determine the actual strain (not micro-strain) given an output voltage as follows.

$$\varepsilon = V_{out} * \left(\frac{4}{V_{br} A K}\right)$$

A sample of data after processing in Excel is shown below (Figure 22).

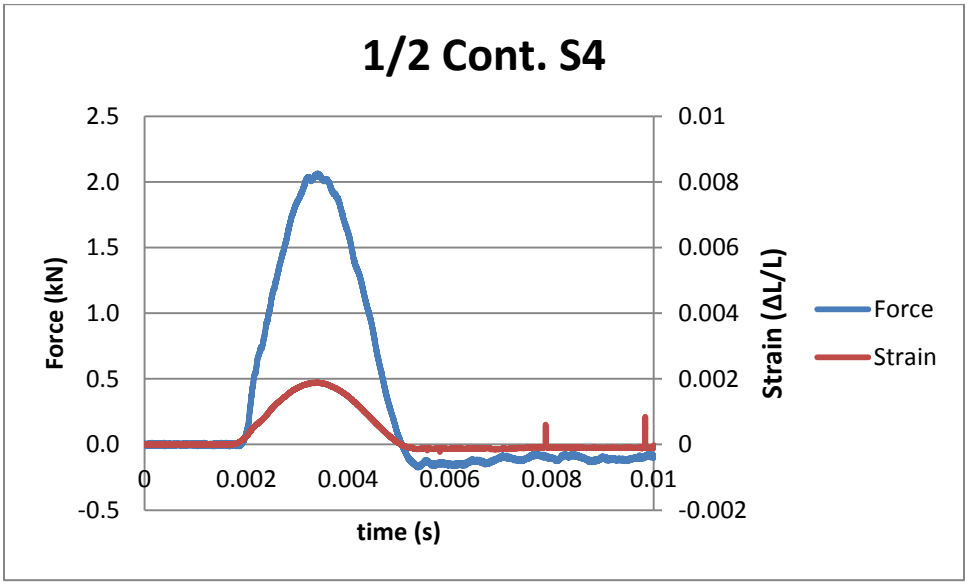

Figure 22 - Sample output from beam testing

As can be seen in the figure above is that the peak force and the peak strain occur at about the same instant. This is to be expected, and for all of the calculations that follow in the section concerning energy absorption, the peaks are assumed to coincide with each other. If there is a temporal difference between peaks, it is assumed to be negligible. Another thing that shows up in the figure is the presence of strain spikes (these can be seen after the impact towards the right of the graph). These are undoubtedly measures of interference experienced by the strain gage. They may be caused by motion in the lead wires, or perhaps magnetic fields caused by the moving

plate relative to the steel support dowel pins upon which the plate rests. In either case, the spikes are cropped in the data analysis to avoid potentially counting a spike as the peak strain for the test.

Results

The results from the simply supported beam testing are similar to the results of the flat plate testing. Shown in the following figures are the results showing the peak forces and strains with associated error bars representing the standard error.

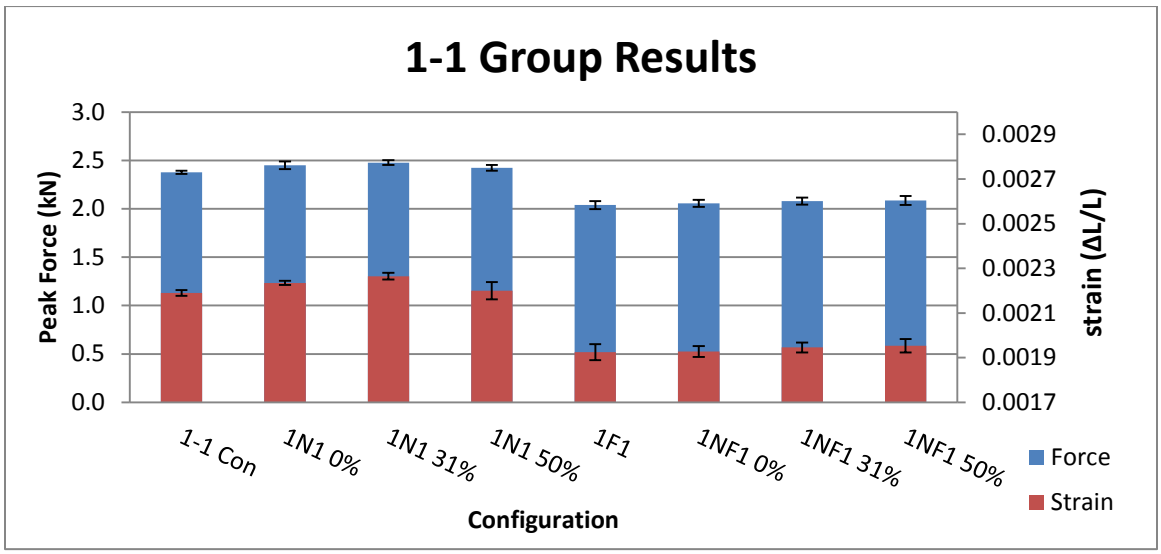

Figure 23 - 1-1 Group results

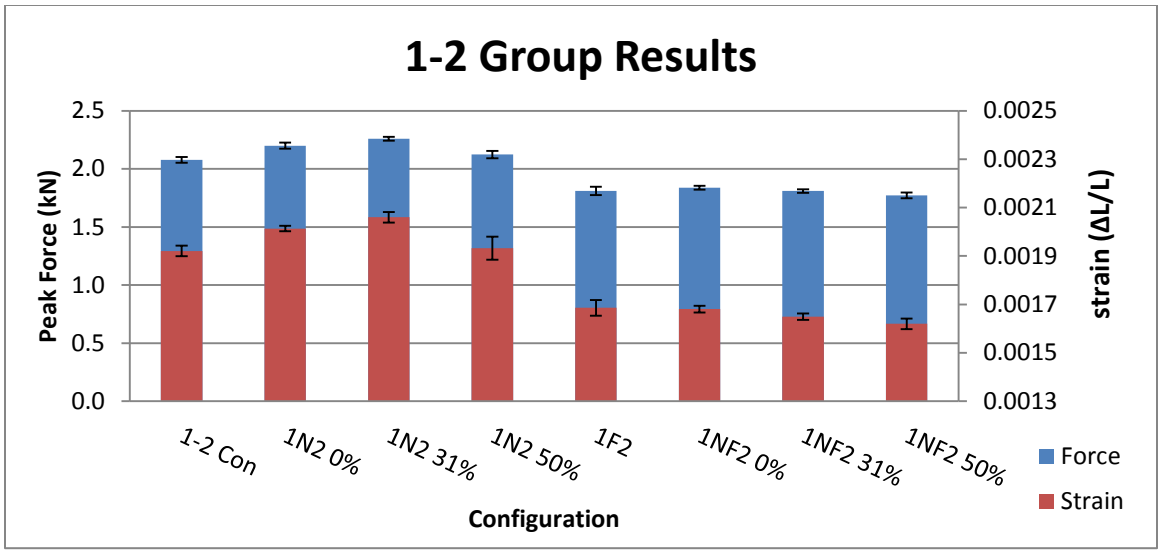

Figure 24 - 1-2 Group results

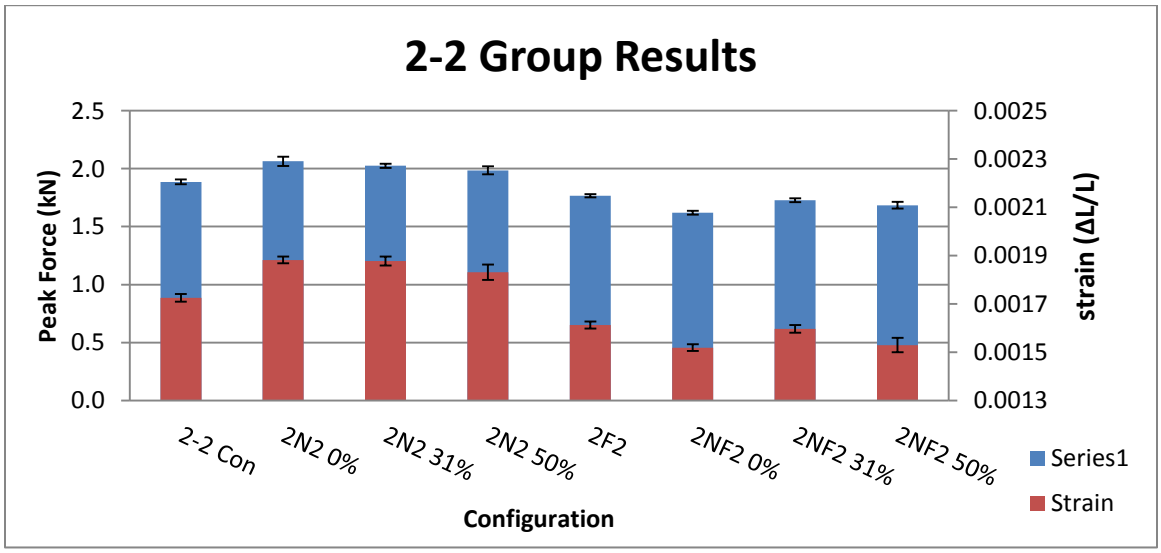

Figure 25 - 2-2 Group results

Just as in the case of the flat plate testing presented in the previous chapter, the results need to be normalized to the thickness of the sample, however since there is more

information gathered in this testing with the strain measurement being recorded, another metric for performance can be used. This metric is the energy absorbed by the mouthguard coupon, and can be calculated using the peak force in conjunction with the strain in the beam. This approach and the results are presented in the next section.

Calculation of Energy Absorbed by Coupon

The force transmitted to the load cell and strain on the beam can be used to calculate the energy absorbed by the coupon. The idea is to use a simple energy balance to arrive at the energy absorbed by the coupon. If the system can be viewed as a simply supported beam subject to a localized distributed force, and at the time of peak force and strain, the situation can be shown as below (Figure 26).

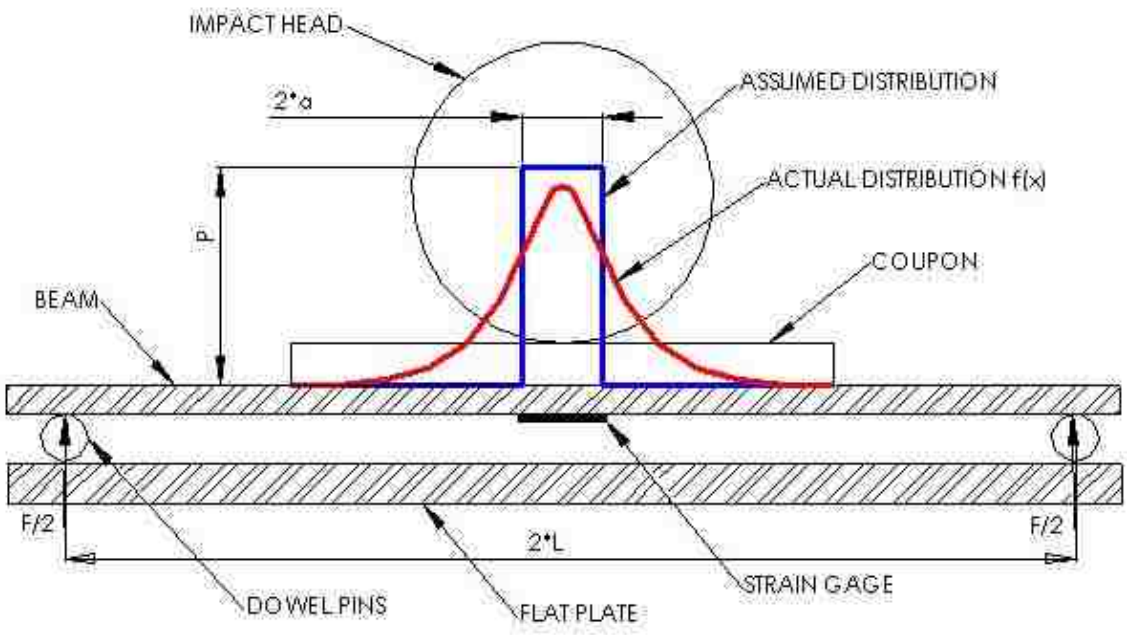

Figure 26 - Simply supported beam under locally distributed force

The load case shown in the figure is idealized. It is difficult to know what the actual load distribution is. What can be done is assume a uniform distribution that is the equivalent in magnitude to the actual distribution. If it is assumed that the actual distribution is $f(x)$, then the following would be true of the idealized uniform force.

$$\int f(x)dx = P * 2a = F$$

By assuming a uniform distributed force, it is possible to calculate the moment across the length of the beam. The beam can be treated as symmetric, and split into two sections; from x = 0 to L-a, and from L-a to L. In the first section, we have the following equation of the moment:

$$M_1 = \frac{Fx}{2} \ for\ 0 < x < (L - a)$$

In the second section of the beam, the moment is as follows:

$$M_2 = \frac{Fx}{2} - \frac{F}{4a}(x + a - L)^2 \ for\ (L - a) < x < L$$

Given the force and strain values gathered in the testing, it is possible to determine the width of the assumed uniform force distribution, a, by using the following equations. From beam theory, we know that the moment in the beam at any given point is as follows:

$$M = \frac{\varepsilon EI}{y}$$

The moment in the center of the beam at the bottom surface may then be calculated using the strain data from the test. Also, M_2 can be evaluated at the center of the beam where

the strain data is taken. These two expressions for the moment at the center of the beam can be equated and used in conjunction with the above expression for P to calculate the width of the effective stress distribution, a. This is the width of the assumed force profile shown in Figure 26.

$$a = 2L - \frac{4\varepsilon EI}{Fy}$$

Where F and ε are determined from the testing, and y is taken as half of the thickness of the aluminum beam. With these values known, the strain energy within the beam at peak load may be calculated next. By taking advantage of the symmetry of the beam and load, the strain energy at peak force and strain can be calculated as such:

$$U = 2\int_0^{L-a} \frac{{M_1}^2}{2EI}\,dx + 2\int_{L-a}^{L} \frac{{M_2}^2}{2EI}\,dx$$

Carrying out the calculation (performed in MATLAB, code is shown in Appendix C), we arrive at the following equation:

$$U = \frac{F^2 a(7a^2 - 20aL + 15L^2)}{60EI} + \frac{F^2(L-a)^3}{12EI}$$

With the strain energy now calculated, the energy absorbed by the mouthguard coupon can be calculated by an energy balance. Another assumption must be made here. The system must be treated as quasi-static for the instant of peak force and deflection. That is, it must be assumed that nothing is moving at this instant, and that all of the kinetic energy of the crosshead has been either absorbed by the coupon or transferred into

strain energy in the beam. Additionally, it is assumed that other sources for energy dissipation (such as sound waves, heat and strain energy in the rest of the equipment) are ignored, and the energy in the system exists exclusively in the test coupon and the beam.

The energy absorbed by the coupon would then be the following:

$$E_c = K - U$$

Where E_c is the energy absorbed by the guard, K is the kinetic energy of the drop tower crosshead prior to contact with the coupon, and U is the strain energy given above. The kinetic energy must be calculated on a test-to-test basis due to the varying thickness of the coupons and is done so as such;

$$K = \frac{mV^2}{2}$$

Where m is the combined mass of the crosshead, impact head and hardware, and V is the velocity of the crosshead at the point when contact with the coupon first occurs. The velocity can be calculated given the coupon thickness and the gauge height at which the crosshead is initially set. From the following energy balance, we can get the velocity.

$$mg(h_g - t) = \frac{mV^2}{2}$$

Where h_g is the gauge height and t is the coupon thickness, and the velocity is:

$$V = \sqrt{2g(h_g - t)}$$

Finally, the energy absorbed by the mouthguard coupon can be calculated as such:

$$E_c = mg(h_g - t) - \frac{F^2 a(7a^2 - 20aL + 15L^2)}{60EI} - \frac{F^2(L-a)^3}{12EI}$$

The next step in this approach is to normalize the energy absorbed by the coupon in terms of the coupon thickness by simply dividing the energy by thickness. Doing this results in the following charts, and is presented as a percentage of the initial system energy (the initial potential energy).

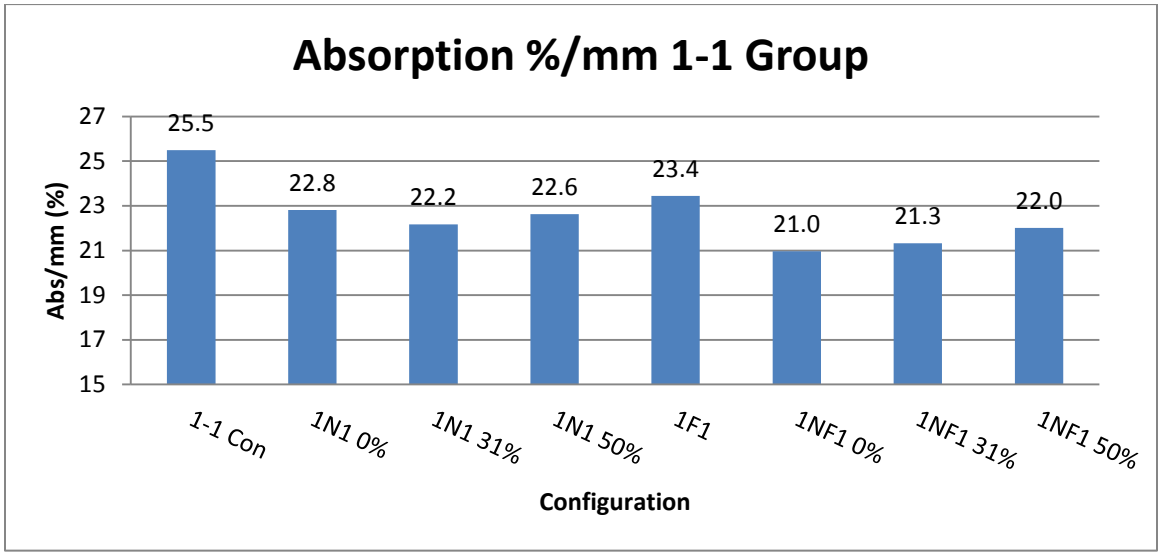

Figure 27 - Absorption %/mm 1-1 group

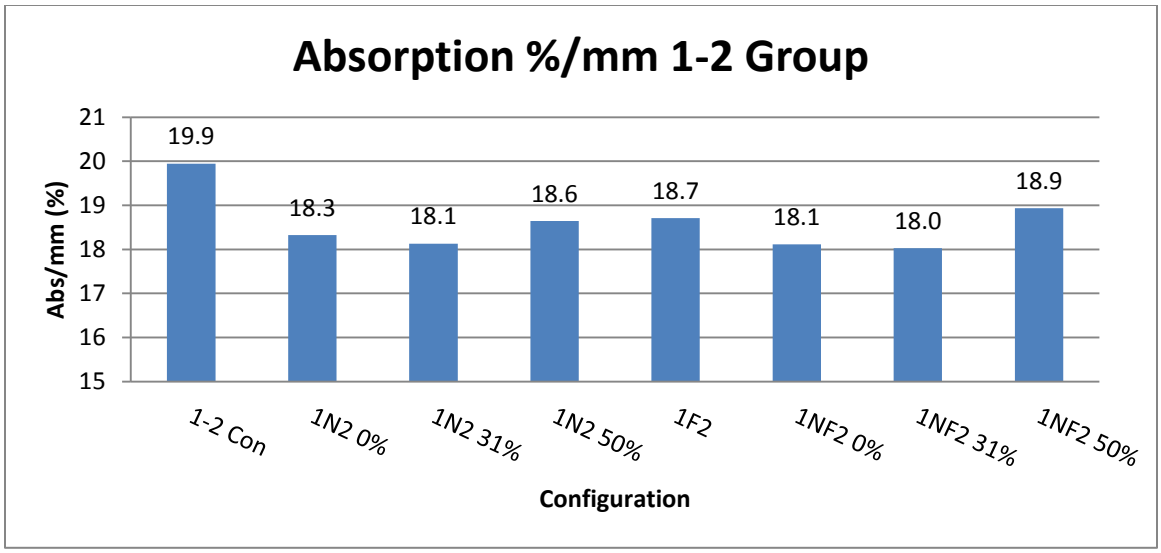

Figure 28 - Absorption %/mm 1-2 group

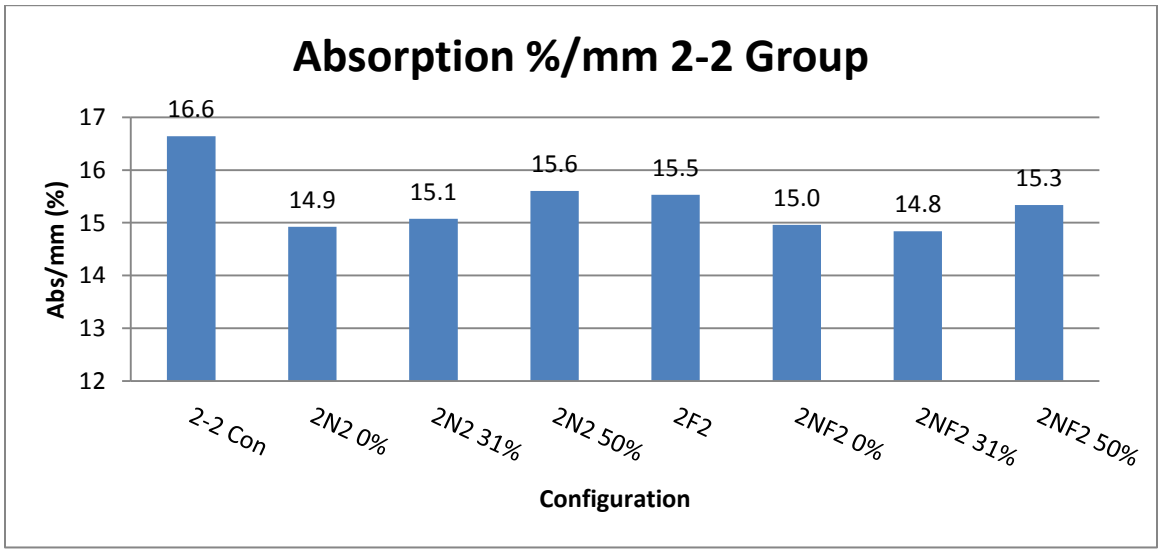

Figure 29 - Absorption %/mm 2-2 group

The above charts can be misleading because it shows that the best performing designs are actually the controls, but this may not be the case. As was done with the flat

plate testing, the performance of each group should be compared to a control of equal thickness, and so a similar procedure is followed and a curve fit is used to determine how an EVA only sample would perform at any given thickness. The novel groups may then be compared to a control of the same would-be thickness. This leads to the following comparisons as shown in the charts below, presented as the percent difference in energy absorbed per mm as compared to a control EVA only of the same thickness.

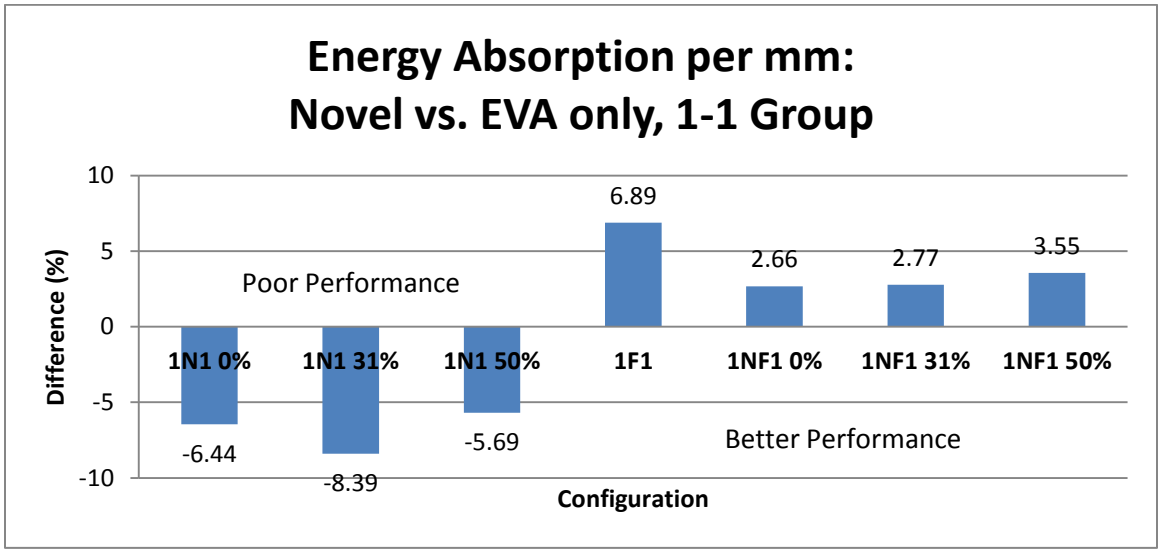

Figure 30 - Absorption per mm: Novel vs. EVA, 1-1 Group

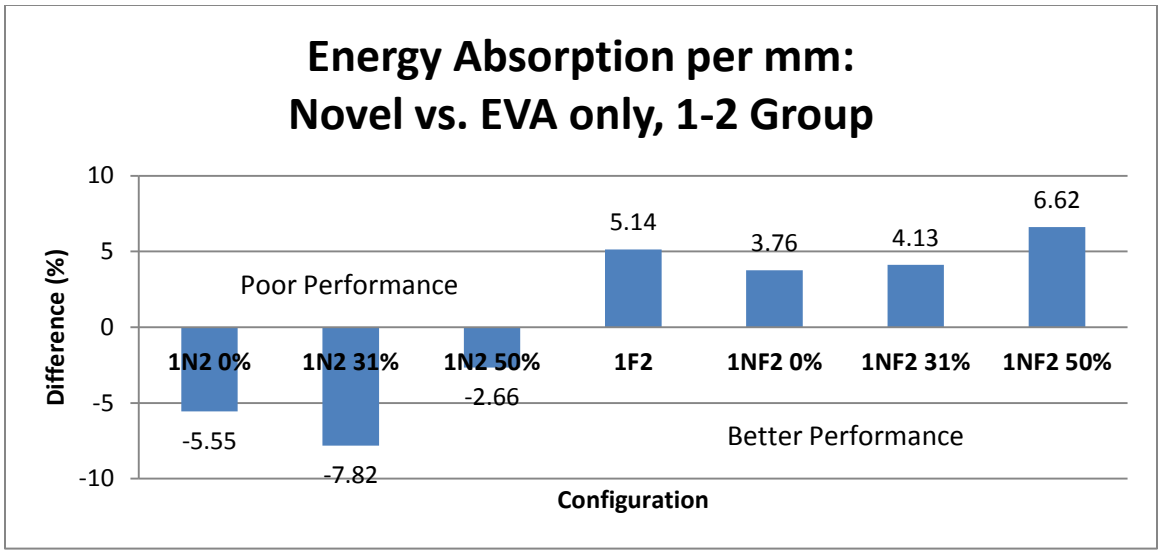

Figure 31 - Absorption per mm: Novel vs. EVA, 1-2 Group

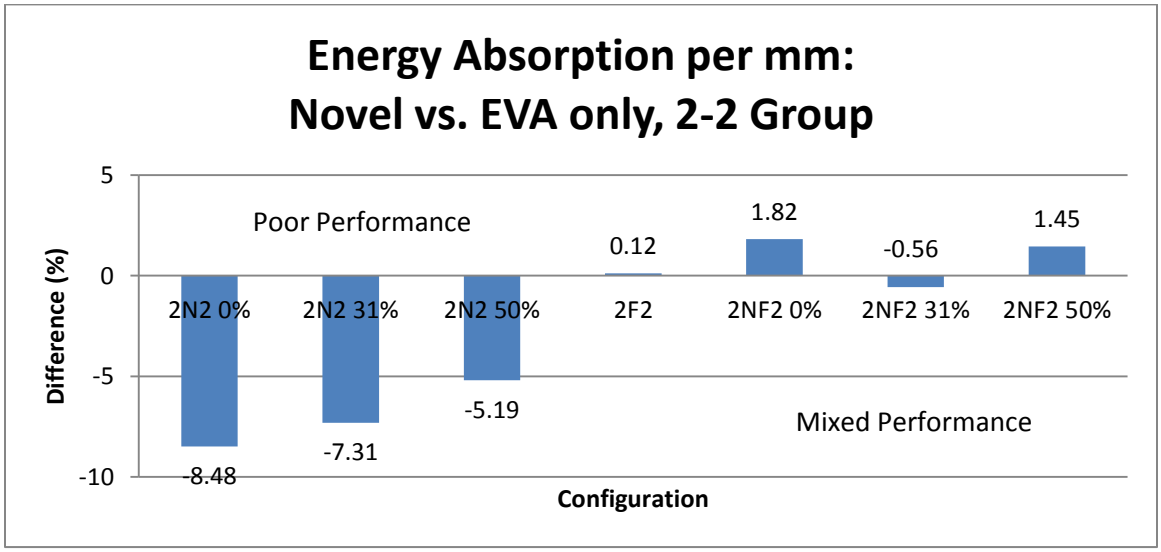

Figure 32 - Absorption per mm: Novel vs. EVA, 2-2 Group

What can be seen in the charts above is a trend similar to that of the flat plate testing; the novel designs incorporating Nitinol only performed poorly in comparison to the controls, and the novel designs that incorporated a foam layer performed only

modestly better than the controls. Another observation is the relative decrease in significant change as the samples get thicker. That is, as more EVA is incorporated into the design, the more it behaves as an EVA only control. The trend remains the same, in that the designs with a Nitinol insert only show decreased performance and the ones that include a foam layer show only modest gains.

The next step in the analysis is to see if these results should be considered significant. To test this, a test between means is conducted using the mean value of energy absorption and standard deviation for each group. This will allow for the calculation of a ratio between the difference of means and the standard error of each paired group. This can be done for each novel configuration versus the control, and between novel configurations. For instance, comparing the novel configurations containing a Nitinol insert can illustrate whether the PAF of the insert makes any difference to the performance. The formula for the ratio of difference to standard error is shown below (Ehrenberg, 1982).

$$ratio = \frac{|\mu_1 - \mu_2|}{\sqrt{\left(\frac{{s_1}^2}{n} + \frac{{s_2}^2}{n}\right)}}$$

Where μ_x is the mean, s_x is the standard deviation and n is the sample size of configuration x (assuming a normal distribution). Carrying out this calculation for each configuration incorporating Nitinol gives the following results.

Abs / mm : 1-1 Group Comparison					
config	**config**	**diff**	**std err**	**ratio**	**signif ?**
1N1 0%	**1N1 31%**	0.0064	0.0039	1.66	maybe
1N1 0%	**1N1 50%**	0.0018	0.0053	0.35	no
1N1 31%	**1N1 50%**	0.0046	0.0051	0.90	no
1NF1 0%	**1NF1 31%**	0.0067	0.0055	1.22	no
1NF1 0%	**1NF1 50%**	0.0083	0.0052	1.59	no
1NF1 31%	**1NF1 50%**	0.0015	0.0063	0.25	no

Figure 33 - 1-1 Group comparison

What can be drawn from this data is that there is no real difference in coupon performance between samples with different inserts. That is the inclusion of the holes, and the number of holes in the Nitinol inserts really make no difference. The results for the 1-2 and 2-2 groups follow the same pattern, and are listed in Appendix D.

Further evidence that the different Nitinol insert designs made no difference can be gathered from a single factor ANOVA. This was performed in Excel, and the results are listed below. The comparisons were made for the 1-N-1 groups and 1-N-F-1 groups.

SUMMARY

Groups	*Count*	*Sum*	*Average*	*Variance*
1N1 0	10	2.280977	0.228098	8.43E-05
1N1 31	10	2.216879	0.221688	6.44E-05
1N1 50	10	2.262524	0.226252	0.000192

ANOVA

Source of Variation	*SS*	*df*	*MS*	*F*	*P-value*	*F crit*
Between Groups	0.000218	2	0.000109	0.959108	0.395909	3.354131
Within Groups	0.003065	27	0.000114			
Total	0.003283	29				

Figure 34 - ANOVA for 1-N-1 groups

SUMMARY

Groups	*Count*	*Sum*	*Average*	*Variance*
1NF1 0	10	2.096788	0.209679	9.11E-05
1NF1 31	10	2.132047	0.213205	0.000212
1NF1 50	10	2.20147	0.220147	0.00018

ANOVA

Source of Variation	*SS*	*df*	*MS*	*F*	*P-value*	*F crit*
Between Groups	0.000567	2	0.000284	1.760547	0.191121	3.354131
Within Groups	0.004351	27	0.000161			
Total	0.004918	29				

Figure 35 - ANOVA for 1-N-F-1 groups

In both cases shown in the tables above, the F-statistic is below the critical value, and the P-value is above the level of significance, which was set to 0.05. It can be

concluded that there is, in fact, no difference within the groups containing the Nitinol inserts.

It is a little more difficult to test for significance when comparing the novel groups to the control group, and an ANOVA test does not make sense because of the difference in thicknesses. What can be done is to graphically compare the novel groups to the control using confidence intervals on the control group. This is done in the following figure.

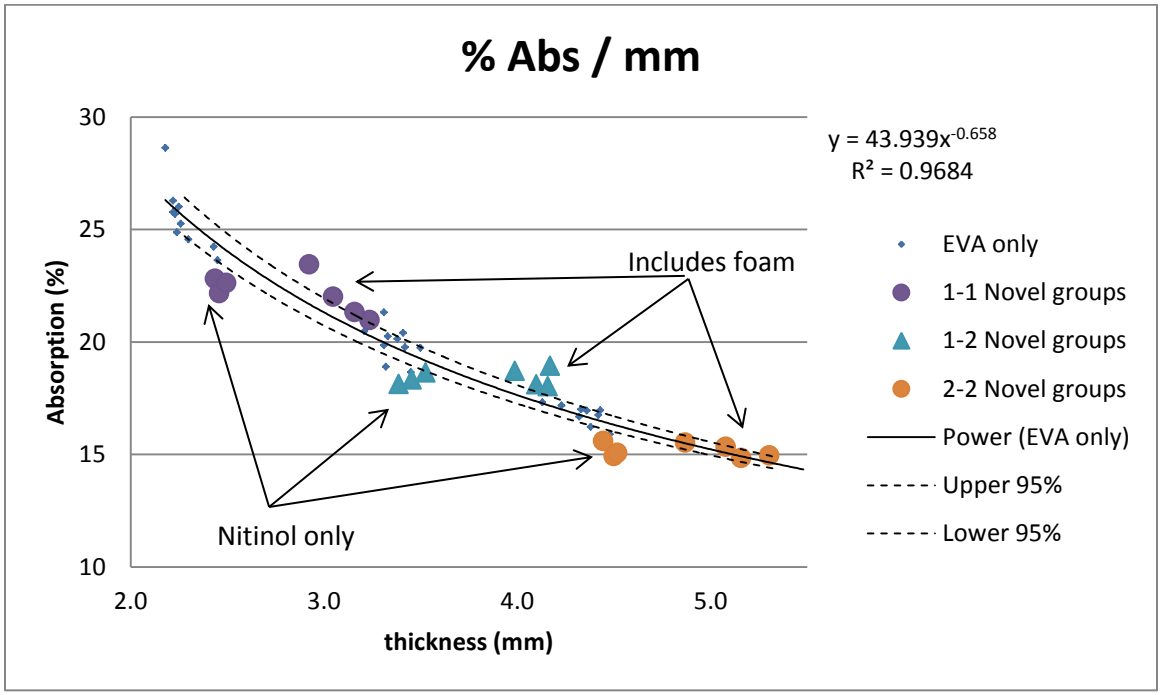

Figure 36 - Confidence interval examination

The central curve fit in this graph (solid line) is generated from the control group data for all thicknesses. The 95% confidence interval lines (dashed) are generated by

calculating the 95% confidence intervals for each control group using the following formula (Ehrenberg, 1982).

$$C = \mu \pm z^* \frac{s}{\sqrt{n}}$$

Where μ is the sample mean, z^* is 1.96 (for 95% confidence level), s is the standard deviation, and n is the sample size (10). The confidence interval lines were created via curve fit (power to match the curve for the entire data set), and extended by one unit to envelope the thicker samples.

What can be seen in the graph is that, in general, all of the novel groups fall near to the envelope of the 95% confidence interval of the control group. That is not to say that there is no statistical difference between the novel and control groups, but there is a chance that there may be none.

What can be done here is a comparison of a novel group to a control group of similar thickness. That is, the 1-N-F-1 groups can be compared to the 1-2 Control group because they have very similar average thickness; 3.36 mm for the control and 3.24 for the 1-N-F-1 0% design. In this case an ANOVA test can be performed with the assumption that the thickness is essentially the same (3.7% difference). Carrying out this analysis gives the following.

Anova: Single Factor

SUMMARY

Groups	*Count*	*Sum*	*Average*	*Variance*
1-2 Con	10	1.994597	0.19946	5.97E-05
1NF1 50	10	2.20147	0.220147	0.00018

ANOVA

Source of Variation	*SS*	*df*	*MS*	*F*	*P-value*	*F crit*
Between Groups	0.00214	1	0.00214	17.86256	0.000508	4.413873
Within Groups	0.002156	18	0.00012			
Total	0.004296	19				

Figure 37 - ANOVA for 1-N-F-1 0% vs. 1-2 Control

This analysis shows that there is, in fact, a statistical difference between the two groups with an F-statistic much larger than F-critical, and a P-value much lower than the prescribed 0.05. With no statistical difference between the other two designs, and similar variances in the 1-N-F-1 group (31% and 50%), it can be inferred that they are also statistically different from the 1-2 Control. The same type of analysis on the 1-F-1 versus the 1-2 Control shows the same thing, with large F-statistic and small P-value. It can be concluded that the differences shown in Figure 30 through Figure 32 are, in fact, real although minor differences.

CHAPTER 5

DISCUSSION, ERROR, OTHER TESTING AND FUTURE WORK

Discussion

The outcome of this study is rather disappointing considering the initial expectation of the novel mouthguard designs. It was posited at the onset of the study that the novel design incorporating the Nitinol and foam layers together would outperform a design incorporating only one of the two components, and furthermore, greatly outperform the control design with EVA only. What has been shown in the previous two chapters is that including a Nitinol insert alone actually lowers the ability of the mouthguard to absorb shock. Given the design of the first test, using only the flat plate, this discovery is not that surprising because the energy absorbing mode in this test is simply compression and the addition of a relatively incompressible material to the design really serves no purpose other than force distribution. It was thought, initially, that by distributing the force of the impact over a larger area of EVA, that the force experienced by the substrate (the load cell) would decrease and that more energy would be dissipated by the increased amount of EVA involved. As it turns out, the data proves just the opposite. It may be that including the Nitinol insert, in effect, eliminates the ability of the underlying EVA to absorb energy and instead creates something of a hard surface that acts as a rigid body. This may be due simply to the EVA's relative inability to compress, because in the case of the Nitinol and foam configurations, the study shows the opposite. In this case, the design actually does perform slightly better.

While the designs with both the Nitinol and foam do perform better than the control, it is surprising that there is just a very modest increase in performance.

Sources of Error

With any experimental design, error is inevitably introduced through any number of sources. In this particular experiment, the sources of error can come from the sensors, the equipment (drop tower), and variations in the coupon materials and, of course, human error. The specifications for the load cell used in this test states a non-linearity of $\leq 2\%$ of full scale, or, ≤ 0.044 kN. (PCB Piezotronics, 2005). Most likely the tests conducted here contain errors due to the load cell on the lower range of this because the range of forces being measures all fall in a relatively compact region of the load cell capacity from about 2.0 to 5.0 kN, which is from 10-25% of its range. One can safely assume that, given the range of testing, that the error from the load cell is most likely no more than about $\pm$ 0.01 kN. Another potential source of error, as it regards to the force measurement, might come from data clipping on the recording end, i.e. the oscilloscope. This might occur if the sample rate was too low for the event being measured. For these tests, the sample rate was 1,000,000 samples/sec, and data clipping is extremely unlikely, making this source of error likely negligible.

More likely sources of error in this experiment are due to variations in the coupon manufacture and variations in the set-up of the drop tower prior to each round of testing. As mentioned in chapter two, some difficulty was encountered during the coupon manufacturing process involving the formations of air pockets in between the various layers of the coupon. This was addressed by piercing two holes at the far ends of the

coupon to allow air to escape during the forming process, but small air pockets were still evident in a few of the coupons. The air pockets (if present in a sample) may act as a shock absorber (Westerman, Stringfellow, & Eccleston, 2002), thus providing an un-accounted for variable in the testing. The other likely source of error involves the set-up of the drop tower itself, and will be discussed more in depth.

Due to the limited number of Nitinol inserts available for testing, the inserts had to be re-used. This, in part, led to the necessity for several rounds of testing, and consequently, several individual set-ups of the drop tower. Prior to each round of testing, whether on the flat plate or on the simply supported beam, the initial height of the crosshead had to be set. This was done using a gauge block as a reference for the nominal 50.8 mm (2.00") drop height. The height of the crosshead is controlled, during repeated tests, using an adjustable Hall-effect sensor which can be moved up or down to set the initial height of the drop. This is adjusted through a trial-and-error process in which the sensor is set, and the crosshead is allowed to return to initial position and then measured using the gauge block. Each set-up requires several attempts to set this initial height, and some variation from the nominal height must be accepted. For this testing, the accepted variation from nominal was less than 0.5 mm, and in general was around 0.25 mm. This would represent an error in potential energy (at 0.5 mm) of 0.021 Joules. While this is a small percentage of the initial energy, it is an unavoidable source of error for the experiment and should be addressed in future work if this test method is to be used.

Another source of error involving the set-up of the drop tower involves the two-piece crosshead. The upper portion of the crosshead is attached to the control mechanism of the machine, and the lower portion is attached to the upper via the interchangeable weight plates. It is possible to misalign the plates while securing the two halves of the crosshead in such a manner as to virtually immobilize the crosshead entirely. This was discovered prior to the fourth round of testing, at which point it was believed that the machine was broken. Assistance showed that the two halves of the crosshead were simply misaligned, and upon alignment, the machine worked properly and the testing resumed. This leads to the suspicion that, depending on how the crosshead halves are aligned, the friction between the crosshead and the guide rods could vary greatly from one round of testing to the next. This variable friction would introduce an unquantifiable loss in kinetic energy during a test and lead to lower force readings.

Both the initial height variation and the possibility of added friction in the crosshead would account for some of the round-to-round variations within the same configuration seen in the results. To further examine the extent to which these variations impact the data, a small study was performed using two coupons from the 1-2 control group (1mm outer and 2mm inner EVA layers). The samples were #1 and #2, chosen arbitrarily. The drop tower was set-up with the flat plate, and all of the routine measures were taken to calibrate the test; the plates were affixed to the crosshead and the initial height was set using the gauge block just like all previous testing. Each sample was tested 10 times and between each test, the sample was removed from the plate (and the two-sided tape), and positioned again for the next test. To simulate a second round of testing, the plates were removed and then reattached, and the gauge block was used to

reset the initial height of the crosshead. The two sided tape was also replaced. The two samples were then tested 10 times following the same routine. The mean peak forces for the two samples for each setup are shown below (Figure 38).

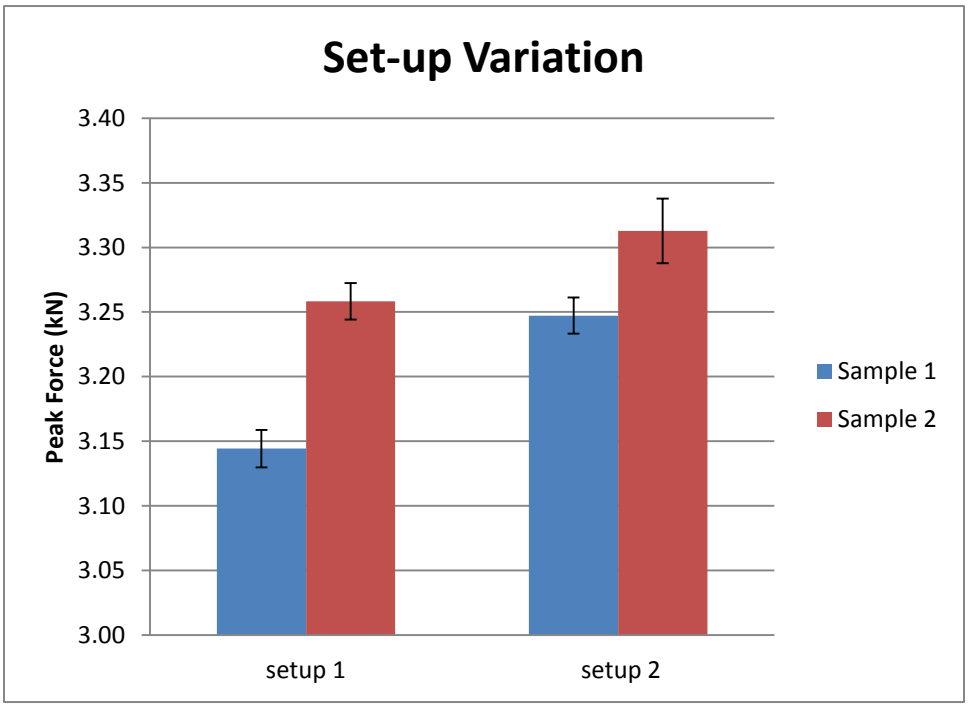

Figure 38 - Setup Variation

What is shown in the figure is that there is a significant difference between the mean peak forces for both samples between the two setups. The error bars in the figure are the standard errors for each individual set of 10 tests, and the significance of the results can be tested by comparing the difference between means to the combined standard error of combined data for each setup following the expression below (Ehrenberg, 1982).

$$error = \sqrt{\left(\frac{{s_1}^2}{n_1} + \frac{{s_2}^2}{n_2}\right)}$$

Where s_x is the standard deviation, and n_x is the sample size. The results of this is shown below.

	Sample 1 (kN)	Sample 2 (kN)
Difference	0.10	0.05
Std error	0.02	0.03

Figure 39 - Setup variation significance

This shows that there is a statistically significant difference between the means of each setup for both samples (the difference is larger than the standard error). It is unclear how much this may have affected the results of this study, but this source of error must be considered confirmed based on this investigation.

One more possible source of error was mentioned earlier in Chapter 4 in the section describing the coupon construction. That is, several of the 50% PAF Nitinol inserts appeared to have broken during the testing. Once this was discovered, special attention was paid to the shape of the force-time curve during the tests with these particular inserts. During one test, in particular, the curve did not look like previous tests, and the coupon was inspected and found to contain a broken insert. At this point, it was concluded that the insert fractured during the test. The force time curve for this test is shown below (Figure 40).

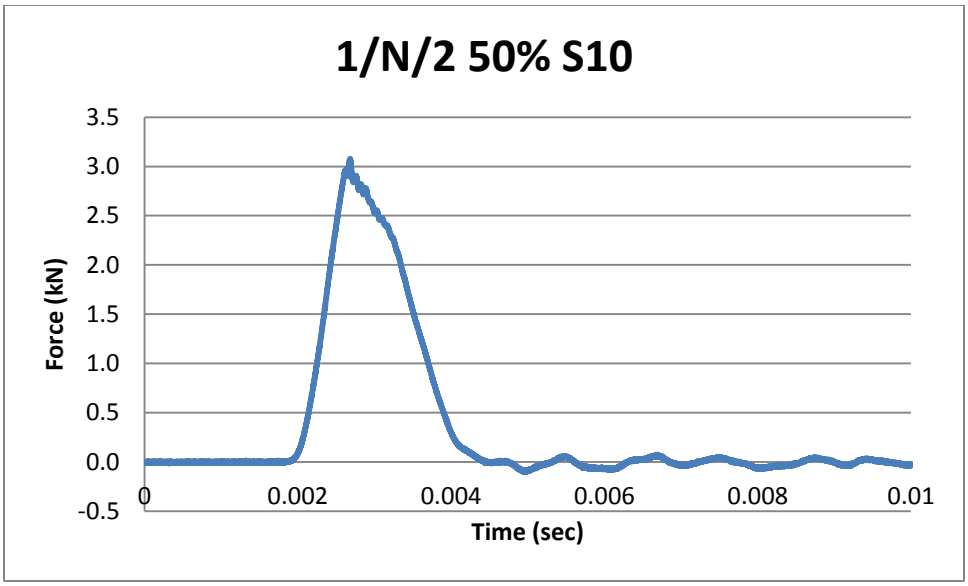

Figure 40 - Example of test with broken insert

The feature that stands out in this graph is the jagged trailing edge of the curve just past the peak, and this was the indicator that the insert may have broken. The peak force for this test was 3.08 kN, and if a nominal value of the contact area is taken to be around 6 mm (this is typical for the testing on the simply supported beam), and the width of the insert is 9 mm, this force would produce a pressure of around 57 MPa. This value is much less than the UTS of the Nitinol used of 1,537.6 MPa, as stated by Memry (Memry GmbH, 2012), however strain rate considerations must be taken into account, and the contact area used assumes a uniform force distribution, which will be lower than the actual peak force that the insert may have experienced during the test. It may be the case, as evidenced by the fractured insert, that the peak pressure within the coupon exceeds the UTS of the Nitinol. This unexpected incident may have added to some of the error in testing, by lowering the peak force recorded by the load cell dissipating the

energy of the impact by fracturing the insert. This phenomenon was posited by Takeda as a possible advantage of using a hard insert (Takeda, et al., 2006), and could be employed as something of a, albeit improbable, fail-safe in future designs.

Additional Testing

As mentioned in the abstract, the use of a 'soft' of 'hard' impact head will vary the way in which the mouthguard performs. This was a theory posed and tested by Takeda (T. Takeda, 2004). It was intended in the work here to include the use of a soft impact head to test this theory in parallel with the testing done with the aluminum impact head. To this end, a baseball was outfitted with a machine nut that could be attached to the crosshead of the impact tower and used in the same fashion as the tests with the aluminum impact head. The baseball used is an official MLB ball (purchased from Dick's Sporting Goods), and was modified by coring out a 19 mm hole down to the polymer core of the ball to accept the machine nut as shown below (Figure 41).

Figure 41 - Baseball and machine nut

The machine nut was then secured to the ball by first soaking the yarn surrounding the area with superglue to stiffen the material, and the nut was ground free of the six corners and roughed up (using a grinder), and finally secured into place using J-B Weld. The idea was to modify only the portion of the ball in contact with the crosshead of the drop tower, reducing the chance of changing its mechanical properties, while providing a secure connection with the machine for repeated use. The final product is shown below (Figure 42).

Figure 42 - Modified baseball

A pilot study was performed following the same methods outlined in chapters three and four. No observable difference was seen in any of the configurations in terms of performance. It would seem that the baseball absorbed the lion's share of the energy

and that any contribution to absorption provided by the mouthguard coupon was negligible. These results led to the abandonment of the baseball as an impact head. It may be the case that at higher energies (higher drop height), that the impact object would make a difference, but this remains outside of the scope of this study.

Future Work

One of the things that this study does not test very well is the ability of the mouthguard to spread an impact force over several teeth. It was hoped that the simply supported beam testing would show that the force is distributed over a larger area for the designs including the Nitinol insert, but this seems to have been largely not the case. A different test design may show just the opposite. It may be possible to strain gage several tooth surrogate models and look at differences that each tooth model experiences during a similar impact. It may be possible to place several cantilevered beams close together with strain gages on the lower surface of the beams and use an energy method similar to the one presented in this paper to calculate the strain energy in each individual beam.

It is hoped that the methods for calculating energy absorption using the techniques presented in chapter six relating to strain energy in a beam may provide a novel and purely objective means to evaluate the performance of future shock absorbing devices. Whether these are mouthguards or other devices meant to protect any given substrate, the objective is the same; identify the best device without introducing subjective error into the test process. Methods presented in chapter two used by previous researchers either introduced a degree of subjectivity or simply lacked the proper equipment to accurately measure the shock absorbing capabilities of what may have been very promising

approaches to the problem of protecting athletes from dental trauma that is prevalent in the sporting arenas across the world. As discussed in the section previous regarding sources of error, it is believed that a more controlled testing environment and better equipment control may lead to a testing method superior to any of the ones employed by previous studies.

APPENDIX A: NITINOL INSERT DESIGNS

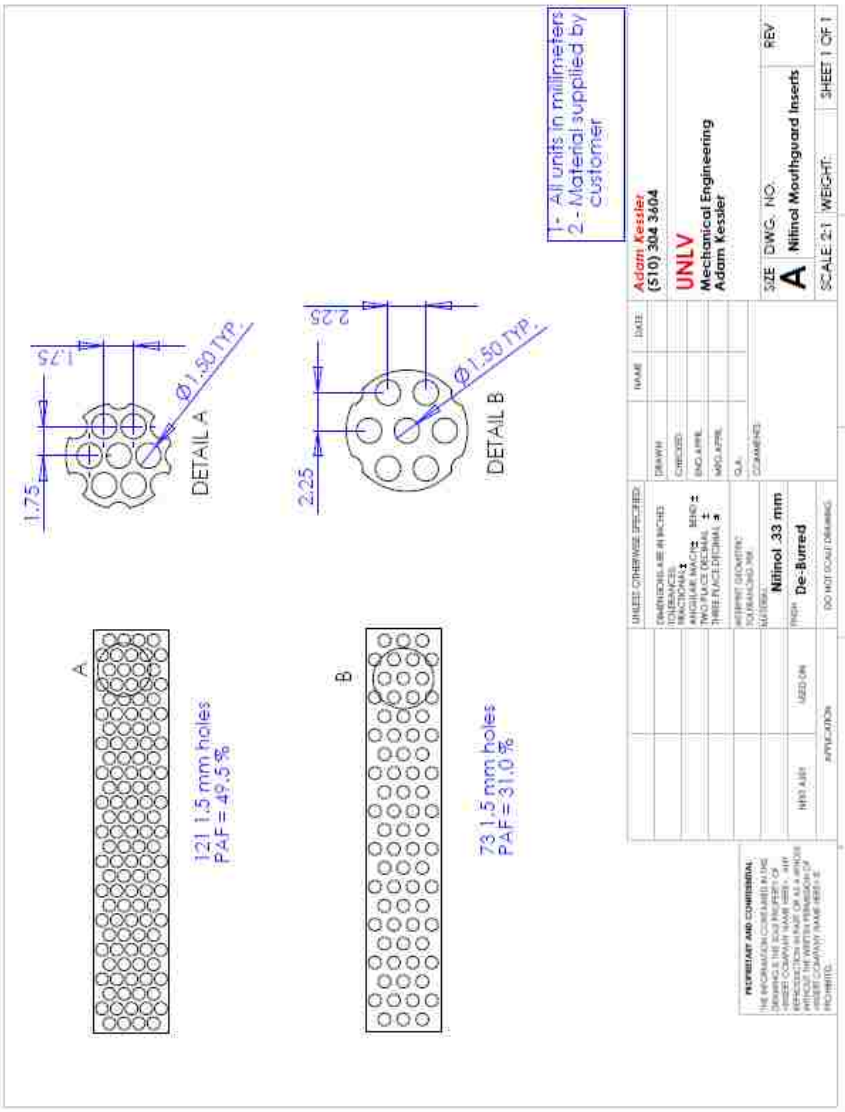

APPENDIX B: FLAT PLATE ASSEMBLY

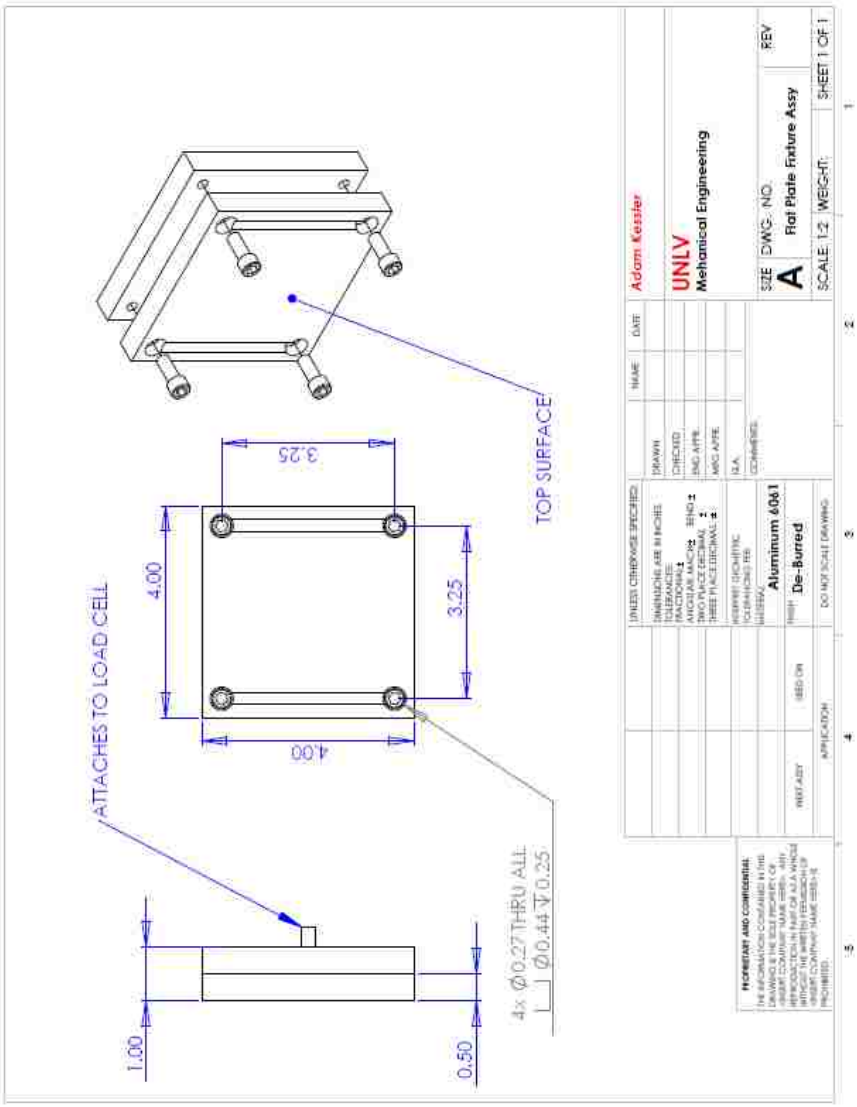

APPENDIX C: MATLAB CODE FOR STRAIN ENERGY

```
clc
clear all

% Strain Energy on simply supported beam with localized distributed
load
%
%                  <---2a---->
%                       F
%                  VVVVVVVVVV
% ================================================
% A                                                A
% <-------------------2L----------------------->

a = sym('a');
L = sym('L');
x = sym('x');
F = sym('F');
M1 = sym('M1');
M2 = sym('M2');
E = sym('E');
I = sym('I');

M1 = F/2*x;
M2 = F/2*x - F/(4*a)*(x+a-L)^2;

U = 2*int(M1^2/(2*E*I),x,0,L-a) + 2*int(M2^2/(2*E*I),x,(L-a),L)

% Below is the output from the previous calculation
% U = (F^2*(L - a)^3)/(12*E*I) + (F^2*a*(15*L^2 - 20*L*a +
7*a^2))/(60*E*I)
```

APPENDIX D: COMPARISON FOR 1-2 AND 2-2 GROUPS

Abs / mm : 1-2 Group Comparison					
config	**config**	**diff**	**std err**	**ratio**	**signif ?**
1N2 0%	**1N2 31%**	0.0020	0.0019	1.02	no
1N2 0%	**1N2 50%**	0.0032	0.0029	1.08	no
1N2 31%	**1N2 50%**	0.0051	0.0030	1.69	maybe
1NF2 0%	**1NF2 31%**	0.0009	0.0058	0.16	no
1NF2 0%	**1NF2 50%**	0.0082	0.0052	1.57	no
1NF2 31%	**1NF2 50%**	0.0091	0.0051	1.77	no

Abs / mm : 2-2 Group Comparison					
config	**config**	**diff**	**std err**	**ratio**	**signif ?**
2N2 0%	**2N2 31%**	0.0015	0.0025	0.61	no
2N2 0%	**2N2 50%**	0.0068	0.0033	2.08	maybe
2N2 31%	**2N2 50%**	0.0053	0.0033	1.61	maybe
2NF2 0%	**2NF2 31%**	0.0012	0.0029	0.43	no
2NF2 0%	**2NF2 50%**	0.0038	0.0030	1.25	no
2NF2 31%	**2NF2 50%**	0.0050	0.0027	1.88	no

REFERENCES

Andrade, R. A., Scabell Evans, P. L., Scabell Almeida, L. A., Rodrigues da Silva, J. d., Lima Guedes, A. M., Guedes, F. R., et al. (2010). Prevalence of dental trauma in Pan American games athletes. *Dental Traumatology*, 248-253.

Bishop, B. M., Davies, E. H., & von Fraunhofer, J. A. (1985). Materials for mouth protectors. *The Journal of Prosthetic Dentistry*, 256-261.

Buslara, Y. R. (1998). Forces transmitted through a laminated mouthguard material with a sorbothane insert. *Endontic Dental Traumatology*, 45-47.

de Wet, F. A., Dent, M., Heyns, M., & Pretorius, J. (1999). Shock absorption potential of different mouth guard materials. *The Journal of Prosthetic Dentistry*, 301-306.

Ehrenberg, A. S. (1982). *A Primer in Data Reduction.* John Wiley and Sons Ltd.

Knapik, J. J., Marshall, S. W., Lee, R. B., Darakjy, S. S., Jones, S. B., Mitchener, T. A., et al. (2007). Mouthguards in sports activities. *Journal of Sports Medicine*, 117-144.

Lunt, D. R., Mendel, D. A., Brantley, W. A., Beck, F. M., Huja, S., Schriever, S. D., et al. (2010). Impact energy absorption of three mouthguard materials in three environments. *Dental Traumatology*, 23-29.

Memry GmbH. (2012, June 29). Certificate of Conformity.

Oikarinen, K. S., Salonen, A. M., & Korhonen, J. (1993). Comparison of the guarding capacities of mouth protectors. *Endontics & Dental Traumatology*, 115-119.

Park, J. B., Shaull, K. L., Overton, B., & Donly, K. J. (1994). Improving mouth guards. *Journal of Prosthetic Dentistry*, 73-80.

Patrick, D. G., van Noort, R., & Found, M. S. (2005). Scale and protection and the various types of sports mouthguard. *British Journal of Sports Medicine*, 278-281.

Patrick, D. G., van Noort, R., & Found, M. S. (2005). Scale of Protection and the Various Types of Sports Mouthguard. *British journal of Sports Medicine*, 278-281.

PCB Piezotronics. (2005, January 25). ICP Force Sensor. *Model Number 200M70*. Depew, New York, United States: PCB Piezotronics.

T. Takeda, e. a. (2004). The Influence of Impact Object Characteristics on Impact Force and Force Absorption by Mouthguard Material. *Dental Traumology*, 12-20.

Takeda, T., Ishigami, K., Handa, J., Naitoh, K., Kurokawa, K., Shibusawa, M., et al. (2006). Does hard insertion and space improve shock absorption ability of mouthguard? *Dental Traumatology*, 77-82.

Vishay Micro-Measurements. (2004, June). 2310A Instruction Manual. *2300 System Signal Conditioning Amplifier*. Vishay Micro-Measurements.

Westerman, B., Stringfellow, P. M., & Eccleston, J. A. (2002). Beneficial effects of air inclusions on the performance of ethylene vinyl acetate (EVA) mouthguard material. *British Journal of Sports Medicine*, 51-53.

Westerman, B., Stringfellow, P. M., & Eccleston, J. A. (2002). EVA Mouthguards: How Thick Should They Be? *Dental Traumatology*, 24-27.

AUTHOR'S CV

Experience

- **Lead Mechanical Engineer: *Bigelow Aerospace**, LLC***
  Las Vegas, NV; 6/06 – 4/08
    - Project Manager for the Galaxy class inflatable module, reporting to the Program Manager for the company.
    - Guided and tracked all mechanical and structural activities related to the spacecraft, including: design changes, test procedures, test articles, mid-fidelity mock-ups, mass budgets, interface control documentation (ICD's), and the day-to-day activities of my staff.
    - Designed the Restraint Layer for the Galaxy spacecraft, including all the necessary analysis, ensured the fit to the craft under operating condition, provided ANSI drawings to the shop, and followed manufacturing through very successful testing.
    - Lead engineer for several projects related to the Sundancer inflatable space module, including: the restraint layer, the Bio-Box payload, the core structure, and docking systems.
    - Co-manager for the mechanical engineering department, and supervised the day-to-day activities of up to twelve engineers, designers and analysts.
    - Interfaced regularly with manufacturing to work through any machining/integration issues.
    - Managed and created all technical drawings and related models using PDMWorks and Solidworks 2006, 2008.

- **Engineering Consultant: *Guidant***
  Santa Clara, CA; 3/06 – 5/06
    - Worked on the VasoView line of endoscopic vessel harvesting systems.
    - Developed a 'duckbill' next generation prototype using their in-house machine shop.

- **Engineering Consultant: *Spinal Kinetics, Inc.***
  Sunnyvale, CA; 1/06 – 3/06
    - Developed and prototyped a delivery system for their spinal implant.

- **Project Engineer: *Aspire Medical, Inc*.**
  Palo Alto, CA; 4/04 – 11/05
    - Responsible for the development of devices to treat Sleep Apnea. – AirFrame™ and Advance™
    - Responsible for building out a small machine shop ground-up.
    - Design and fabrication of fatigue test equipment.

- Complete manufacturing responsibilities; component updates, change orders, quality control, build records (lot histories and documentation), packaging, and clean-room support.
- Solo and accompanied human clinical case support in Belgium and Germany.
- Surgical experience with minimal supervision, at Lychron, LLC.

- **R&D Engineer:** ***Ventrica, Inc.***
  Fremont, CA**;** 10/2000 – 2/2004
  - Distal cardiac bypass anastomotic device - MVP™ System
  - Responsible for the development of novel anastomotic devices for cardiac bypass surgery.
  - Extensive machining and prototyping duties, with heavy emphasis in micro-machining and fabrication.
  - Design and fabrication of various test apparatus, both related to magnetic field measurement, and mechanical validation equipment.
  - Manufacturing support; inspection drawings, process instructions, and product transfer from research and development to production.

Computer / Machine Experience

- SolidWorks (10 years), PDMWorks (2 years), Microsoft Office, ManufactPro, SurfCAM,.
- Capable machinist; Lathes, Mills, CNC programming and machining.

Education

University of Nevada, Las Vegas: 2010 – Present

University of California, Berkeley: B.S.M.E. 1997 - 2000